

2009

Reorganization of Ia Afferent Synapses on Motoneurons after Peripheral Nerve Injuries

Haley E. Titus
Wright State University

Follow this and additional works at: https://corescholar.libraries.wright.edu/etd_all



Part of the [Anatomy Commons](#)

Repository Citation

Titus, Haley E., "Reorganization of Ia Afferent Synapses on Motoneurons after Peripheral Nerve Injuries" (2009). *Browse all Theses and Dissertations*. 937.
https://corescholar.libraries.wright.edu/etd_all/937

This Thesis is brought to you for free and open access by the Theses and Dissertations at CORE Scholar. It has been accepted for inclusion in Browse all Theses and Dissertations by an authorized administrator of CORE Scholar. For more information, please contact library-corescholar@wright.edu.

Reorganization of Ia afferent synapses on
motoneurons after peripheral nerve injuries

A thesis submitted in partial fulfillment
of the requirements for the degree of
Master of Science

By

HALEY ELIZABETH TITUS
B.A., Miami University of Ohio, 2007

2009
Wright State University

WRIGHT STATE UNIVERSITY
SCHOOL OF GRADUATE STUDIES

June 11, 2009

I HEREBY RECOMMEND THAT THE THESIS PREPARED UNDER MY SUPERVISION BY HALEY ELIZABETH TITUS ENTITLED Reorganization of Ia afferent synapses on motoneurons after peripheral nerve injuries BE ACCEPTED IN PARTIAL FULFILLMENT OF THE REQUIREMENTS FOR THE DEGREE OF Master of Science.

Francisco J. Alvarez, Ph.D.
Thesis Director

Timothy Cope, Ph.D.
Department Chair

Committee on
Final Examination

Francisco J. Alvarez, Ph.D.

Timothy Cope, Ph.D.

Mark Rich, Ph.D.

Joseph F. Thomas, Jr., Ph.D.
Dean, School of Graduate Studies

ABSTRACT

Titus, Haley E. M.S., Department of Neuroscience, Cell Biology, and Physiology, Wright State University, 2009. Reorganization of Ia afferent synapses on motoneurons after peripheral nerve injuries.

After peripheral nerve injuries patients lose and do not recover the stretch reflex which leads to altered locomotor function. The focus of this thesis is to investigate the structural integrity of the central connection between Ia afferents and alpha motoneurons that mediate the stretch reflex. The overall hypothesis is that the density and distribution of Ia synapses on motoneurons is altered after peripheral nerve injuries. Analysis of Ia afferent-motoneuron contacts, revealed by vesicular glutamate transporter 1 (VGLUT1) immunoreactivity, on the soma and dendritic arbor of motoneurons after peripheral nerve injuries revealed major reorganizations in the distribution and density of Ia synapses. Synaptic stripping of Ia afferent synapses occurred on the soma and proximal dendrites and appeared to be permanent even after reinnervation; in contrast, VGLUT1 synapses on distal dendrites were unchanged. In conclusion, after peripheral nerve injuries motoneurons are contacted by fewer Ia synapses and they are more distally located. This overall reorganization likely weakens the input and may contribute to stretch reflex anomalies.

Table of Contents

Abstract	iii
Table of Contents	iv
List of Figures	vi
Acknowledgements	vii
I. Introduction	1
II. Background	3
A. Topography of lumbar spinal cord motor pools	3
B. Alpha Motoneuron Anatomy	
1. Soma and Dendritic Arbor	4
2. Synapses	5
C. Ia afferents and muscle spindles	
1. Overview of muscle spindles	6
2. Physiology of Ia-motoneuron synapses	7
3. Ia afferent projections in the spinal cord	8
D. Location of Ia afferent synapses on motoneurons in the lumbar spinal cord	8
E. VGLUT1 as a tool to recognize Ia afferent synapses	
1. What is VGLUT1?	10
2. VGLUT1 as a specific marker of proprioceptive synapses	11
F. Effects of peripheral nerve injuries	
1. Synaptic stripping of motoneuron synaptic contacts	13
2. VGLUT1 contacts on alpha motoneurons in the spinal cord	17
3. The monosynaptic reflex	17
G. Physiological recovery from peripheral nerve injury	
1. Motor unit recruitment	18
2. Differences between self and cross reinnervation	19
3. Time course of reinnervation in the cat and rat	19

4.	Appropriate and inappropriate proprioceptive input in muscle after reinnervation	20
5.	Loss of the stretch reflex	20
III.	Aims	23
IV.	Materials and Methods	25
A.	Surgical Procedures	25
B.	Tissue preparations for analysis	29
C.	Imaging and Analysis	31
V.	Results	36
A.	Aim 1: Changes in VGLUT1 density around the cell soma of NeuN-labeled tibial pool motoneurons	36
B.	Aim 2: Changes in VGLUT1 density around the cell soma of retrogradely labeled MG motoneurons	47
C.	Aim 3: Changes in density of VGLUT1 contacts around the dendrites of retrogradely labeled MG motoneurons	60
VI.	Discussion	70
A.	Methodological Considerations	
1.	VGLUT1 as an effective marker of control and injured Ia afferent synapses	70
2.	Large reductions in NeuN-labeled motoneuron versus MG retrogradely labeled motoneurons	71
3.	Extent of dendritic analysis	71
B.	VGLUT1 contacts on the cell bodies of motoneurons are depleted after peripheral nerve injuries and do not recover	72
C.	Reorganization of VGLUT1 contacts on the dendritic arbor	74
D.	Correlation of VGLUT1 contacts with the physiological changes observed in the Ia-motoneuron connection after peripheral nerve injury and regeneration	76
	Bibliography	79

List of Figures

Figure 1. Vesicular Glutamate Transporter (VGLUT1) Immunoreactivity (IR)	37
Figure 2. Neuronal Nuclear Protein-IR (NeuN-IR)	39
Figure 3. VGLUT1-IR and NeuN-IR for motoneurons within tibial motor pools	43
Figure 4. VGLUT1 contact densities on the cell soma of motoneurons in the Tibial motor pools	45
Figure 5. Dual retrograde labeling for identification of appropriately reinnervated MG motoneurons.	48
Figure 6. Electromyography for reinnervated dual labeled MG motoneurons.	51
Figure 7. Density of VGLUT1 contacts on the soma of reinnervated MG motoneurons after tibial nerve cut and resuture.	53
Figure 8. Density of VGLUT1 contacts on the soma of reinnervated MG motoneurons after MG nerve cut and resuture	55
Figure 9. 3D Analysis of Motoneuron VGLUT1 contacts	61
Figure 10. Motoneuron soma and dendritic arbor reconstructions showing VGLUT1 contacts	63
Figure 11. Density of VGLUT1 contacts on the soma of reinnervated MG motoneurons after tibial nerve cut and resuture	67

Acknowledgements

I would like to express my appreciation for Dr. Francisco Alvarez. He is always optimistic and has been a wonderful teacher and mentor. With his guidance I have gained experience at the bench and in writing that will build the foundation for my future as a neuroscientist. I would like to thank the other members of my committee, Dr. Mark Rich and Dr. Timothy Cope, for their input and support of my project.

I would like to thank the entire Alvarez Lab for helping me learn new techniques at the bench. In addition, I would like to thank the entire Cope Lab for their collaborative efforts on this project and the excitement all members brought to every experiment.

I would like to acknowledge Erin Fulchiero for offering encouragement on a daily basis and being a great friend this past year. I would like to thank my entire extended family for encouraging me to work hard and have a passion for what I am trying to accomplish. Lastly, I would like to express gratitude for my loving boyfriend Chris Mitchell who has spent a good deal of his free time accompanying me in lab during the evenings and over the weekends for the past year. He has really come to embrace neuroscience and I get excited telling him all about it.

I. Introduction

The stretch evoked synaptic potential (SSP) is lost after peripheral nerve injury despite presence of Ia monosynaptic excitatory postsynaptic potentials (EPSPs) on motoneurons (Cope et al., 1994; Haftel et al., 2005). This areflexia results in altered locomotor activity patterns due to the loss of proprioceptive feedback from muscle spindle receptors in the regulation of interjoint coordination and muscle stiffness (Abelew et al., 2000; Maas et al., 2007). As a result the recovery of motor function is incomplete even after successful reconnection and regeneration of injured peripheral nerves. The finding that Ia afferents regenerate peripherally and recover normal sensitivity to stretch leads to the hypothesis that suppression of Ia afferent inputs occurs centrally (Haftel et al., 2005), but the exact mechanisms remain unknown.

It is well known that after peripheral nerve injuries, synapses on axotomized motoneurons are first lost in a phenomenon denominated “synaptic stripping” and then recovered after motoneurons reconnect with muscle. The possibility that this process results in major structural synaptic remodeling and alteration of the composition of inputs to motoneurons has not yet been studied in detail. For example, no anatomical study to date has specifically analyzed the exact fate of Ia synapses, many of which arise from afferents that have been peripherally injured. This thesis explores the possibility that failure in Ia to motoneuron neurotransmission during stretch evoke activity is due in part to a central structural reorganization of Ia synapses on motoneurons. Our overall

hypothesis is that the density and distribution of Ia synapses on motoneurons is altered after peripheral nerve injuries. We also investigated whether possible reorganizations are permanent or otherwise changed when there is successful regeneration in the periphery compared to situations with no peripheral regeneration.

To test this possibility we analyzed Ia afferent-motoneuron contacts, revealed by vesicular glutamate transporter 1 (VGLUT1) immunoreactivity as a proprioceptive marker on the soma and dendritic arbor of motoneurons after peripheral nerve injuries. We injured both motoneurons axons and Ia afferents by transection of the tibial nerve. In some animals the tibial nerve cut ends were resutured to allow regeneration to occur; however, in others the proximal end was ligated to impede peripheral regeneration. The Ia-motoneuron synapses were then analyzed at various post-injury times in lumbar motoneurons that successfully reinnervated the periphery and in others that did not. Therefore, most of the study was focused on tibial nerve motor pools and more specifically on medial gastrocnemius motoneurons.

We concluded that after peripheral nerve injuries there are major reorganizations in the distribution and density of Ia synapses over motoneurons and these changes appear to be relatively permanent. These anatomical analyses are compared to current physiological data to aid in understanding the absence of the stretch evoked synaptic potential (SSP) after peripheral nerve injury.

II. Background

A. Topography of lumbar spinal cord motor pools

The rat lumbar spinal cord is organized cytoarchitecturally in ten lamina. The dorsal horn consists of lamina I through lamina VI (Molander et al., 1984). The focus of this study was on lamina VII and lamina IX in the ventral horn of the spinal cord (Molander et al., 1984). Lamina VII contains the distal dendrites and lamina IX the cell bodies and proximal dendrites of motoneurons. Within lamina IX we focused particularly on the regions containing motor pools which send axons through the tibial and medial gastrocnemius nerve. These regions also contain the ventral projections of sensory proprioceptive afferents injured by the nerve transections performed in this study.

The sciatic nerve gives off articular branches (*rami articulares*) and muscular branches (*rami musculares*). The focus of this study was on a muscular branch, the tibial nerve, and a branch of the tibial nerve, the medial gastrocnemius nerve (Moore et al., 2006). In the rat lumbar spinal cord, tibial nerve motoneurons comprise 49% of all sciatic motoneurons; in contrast, the medial gastrocnemius (MG) motoneuron pool represent only 7% of the total sciatic motoneuron population (Swett et al., 1986). Using retrograde tracing with horseradish peroxidase (HRP) it was found that medial gastrocnemius motoneurons are distributed in a rostro-caudal column that extends from Lumbar 3 (L3) / Lumbar 4 (L4) junction through Lumbar 5 (L5) (Nicolopoulos-Stournaras et al., 1983) and into rostral Lumbar 6 (L6) (Swett et al., 1986). A range of motoneuron sizes was observed: smaller motoneurons were considered gamma

motoneurons (11-30 μm mean diameter), while medium (25-30 μm mean diameter) and large (32-45 μm mean diameter) alpha motoneurons, with the largest at 58 μm mean diameter (Swett et al., 1986).

B1. Alpha Motoneuron Anatomy: Soma and Dendritic Arbor

It is important to note that 95% - 97% of the membrane surface area of motoneurons is located in the dendritic arbor (Fyffe, 2001; Luscher et al., 1992). The total membrane area of a cat hind limb alpha motoneuron can range from 250,000 to 750,000 μm^2 ; the soma only constitutes 6,000-15,000 μm^2 (Luscher et al., 1992). The dendritic arbor of cat alpha motoneurons in the lumbar spinal cord is radial (Fyffe, 2001; Luscher et al., 1992) and can extend up to 1600 μm from the soma in the rostro-caudal direction; extending into the ventral horn and reaching as dorsal as lamina V or VI (Brown et al., 1981). Fully reconstructed hind limb motoneurons of the cat have 7-18 primary dendrites and usually branch up to the 4th or 6th order (Brown et al., 1981).

Only one study performed similar detailed analysis on fully labeled dendritic arbors in triceps surae adult rat motoneurons (Chen et al., 1994). In comparison with cat, rat triceps surae motoneurons had smaller average surface areas (150,000 μm^2 vs. 560,000 μm^2), fewer primary dendrites (8 vs. 12), and shorter total dendritic lengths (36mm vs. 105mm). However, there was not a species difference in number of contacts on the dendritic arbor; therefore, hindlimb rat motoneurons had more contacts per unit of dendritic length (Chen et al., 1994).

For all cat motoneurons, the mean diameter of the stem dendrite and the mean diameter of the cell body share a strong relationship (Luscher et al., 1992). In the hind

limb cat motoneurons, the diameter of the stem dendrite was correlated positively with the dendritic membrane area, the combined dendritic length, and the number of terminations (Luscher et al., 1992). Similarly, in hindlimb rat motoneurons diameter of the stem dendrite was also positively correlated with combined dendritic length, surface area, and volume (Chen et al., 1994).

B2. Alpha Motoneuron Anatomy: Synapses

The complexity of a motoneuron dendritic arbor is proportional to the number of synaptic contacts received (Luscher et al., 1992). Of the estimated 50,000 synaptic inputs on the cat alpha motoneuron, the soma contain 1 - 2% but they occur at relatively high densities, 10-12 synapses per 100 μm^2 (Fyffe, 2001). Proximal dendritic synaptic density (first 100 μm) is equal to or slightly higher than the synaptic density of the soma. Synaptic density declines up to 20 to 30% with increasing distance from the soma (Fyffe, 2001). Several classes of boutons have been defined on motoneuron cells bodies and dendrites. S-type (for spherical vesicles) boutons are considered to be excitatory with 94% of boutons labeled for glutamate (Fyffe, 2001). S-type boutons (for spherical vesicles) represent 20-30% of all somatic boutons, 30% of the proximal dendritic boutons, and 60% of the distal dendritic boutons (Fyffe, 2001). F-type boutons (F for flattened vesicles) are inhibitory and represent approximately around 60% of boutons on somata and proximal dendrites and their density and proportions to all synapses decrease with distance from the soma. There are also other more specialized classes of synapses on motoneurons like C-terminals and M-terminals which occur in lesser proportions (Fyffe, 2001).

M synapses in particular are large boutons with spherical vesicles that receive presynaptic axoaxonic synapses and were demonstrated to originate from dorsal root afferents (Conradi, 1969). These terminals were initially considered to be the electron microscopy (EM) correlate of Ia afferent synapses; however, after these were intraaxonally filled with HRP and analyzed with electron microscopy it was shown that most Ia synapses on motoneurons have a typical S-type morphology (Conradi et al., 1983; Fyffe et al., 1984). Therefore, M synapses could be some Ia afferent S-type synapses that are particularly large. Ia synapses, as the ones that will be reviewed below regarding synaptic stripping, cannot be unambiguously identified without some specific means of labeling them because most Ia afferent synapses are structurally indistinguishable from S-type synapses.

Including all synapses mentioned above, overall synaptic density decreases proximo-distally along the dendritic arbor but the proportion of synapses that are excitatory increases from soma to distal dendrites. The distribution of Ia afferent synapses is believed to follow a similar pattern to the S-type excitatory synapses (and M-synapses); however, Ia afferents only contribute a small portion of all excitatory synapses targeting the motoneuron.

C1. Ia afferents and muscle spindles: Overview of muscle spindles

Muscle spindles act as stretch receptors by encoding information about muscle length; containing 8-10 intrafusal muscle fibers and are in parallel with extrafusal muscle fibers (Purves et al., 2008). The sensory component of the muscle spindle contains two types of endings that contribute to the monosynaptic stretch reflex. The primary

(annulospiral) endings give rise to the Ia afferent fibers and the secondary endings give rise to the group II afferent fibers (Luscher et al., 1992).

C2. Ia afferents and muscle spindles: Physiology of Ia-motoneuron synapses

The circuit of the monosynaptic stretch reflex is the connection of the large diameter Ia afferent from an intrafusal muscle spindle to the alpha motoneuron in the ventral horn of the spinal cord and the connection of the alpha motoneuron in the ventral horn of the spinal cord with the extrafusal fibers of the homonymous muscle (Purves et al., 2008). In this study the circuit included the Ia afferents from the triceps surae muscles (MG, LG, and Soleus), the motoneurons in tibial motor pools lamina IX of the lumbar spinal cord, and the extrafusal fibers of the triceps surae muscles (MG, LG, and Soleus).

Electrical stimulation of a skeletal muscle nerve activates groups of Ia afferents which produce a composite excitatory postsynaptic electrical potential (EPSP) on motoneurons (Cope et al., 2001). The peak amplitude of the composite EPSP can be equated to synaptic strength and induces a proportional increase in motoneuron firing (Cope et al., 2001). Stimulation frequency plays a role in the composite EPSP amplitude at Ia-MN synapses. At low frequency stimulation (< 1 pps) the amplitude of the composite EPSP remains steady with repeated stimuli and the maximum amplitude of a composite EPSP is defined as the steady-state synaptic strength (Cope et al., 2001). At high frequency stimulation, the amplitudes of composite EPSPs can increase or decrease due to variations in the properties of specific Ia-MN synapses, such as the probability of neurotransmitter release. For example, the composite EPSP of synaptic connections with

low probability of release usually increase during high frequency stimulation (Cope et al., 2001).

C3. Ia afferents and muscle spindles: Ia afferent projections in the spinal cord

The focus of this study is on the synaptic contacts between Ia afferent fibers and motoneurons that form the basis of the monosynaptic stretch reflex. The stem axon of the Ia afferent bifurcates in the dorsal columns shortly after entering the spinal cord into ascending and descending branches (Luscher et al., 1992). The ascending branch of the Ia afferent in the cat has a larger diameter (5.8 μm) compared with the descending branch diameter (3 μm) (Ishizuka et al., 1992). In the cat, a total of 5-11 collaterals are given off from the ascending and descending branch at different rostro-caudal locations (Ishizuka et al., 1979). The collaterals pass through the medial half of the dorsal horn before traveling through the deeper grey matter (Ishizuka et al., 1979). The terminal arborizations of the Ia afferent collaterals occur in medial lamina V, and throughout lamina VII (region of postsynaptic Ia inhibitory interneurons and motoneuron distal dendrites), and lamina IX (motor nuclei region) (Brown et al., 1978; Ishizuka et al., 1979; Luscher et al., 1992). The highest number of Ia afferent terminal branches is found in lamina IX and the lowest number in lamina VII (Ishizuka et al., 1979).

D. Location of Ia afferent synapses on motoneurons in the lumbar spinal cord

Intracellular fills with horseradish peroxidase of Ia afferent fibers and motoneurons coupled with electrophysiology recordings demonstrated that group Ia afferents make synaptic contacts preferentially on the dendritic arbor of alpha

motoneurons in cat (Burke et al., 1979). A single Ia afferent collateral makes contact with 50-60 motoneurons (Brown et al., 1978) with an average of 10 Ia afferent synaptic contacts per motoneuron (range 3-32) (Fyffe, 2001; Luscher et al., 1992). The number of synaptic contacts made by a specific Ia afferent collateral is dependent upon the distance between the motoneuron and the entry point of the Ia afferent (Luscher et al., 1992), such that there are more synaptic contacts on motoneurons located at segmental levels close to the dorsal root entry point of the afferent.

More than 90% of Ia synapses on motoneurons occur on the dendritic arbor, and the highest number (60%) occurs along rostrocaudally-oriented dendrites (Fyffe, 2001). Fewer Ia fiber synaptic contacts (8%) occur along dendrites oriented in the dorsolateral to ventromedial axis (Burke et al., 1996). Dendrites oriented in the dorsomedial-ventrolateral axons are parallel to the trajectory of Ia afferent collaterals and receive 22% of all contacts. Overall Ia synapses have been estimated to contribute between 1-2% of all synaptic inputs (500-1,000 synapses) to the adult cat motoneuron (Burke et al., 1996).

MG Ia afferent fibers contact a larger percentage of homonymous (100%) than heteronymous (66%) motoneurons (Scott et al., 1976). Larger EPSPs are recorded from homonymous motoneurons (Cope et al., 2001; Scott et al., 1976). This suggested possible differences in synapses formed by homonymous or heteronymous Ia afferent on MG motoneurons including greater release of transmitter (presynaptic) and/or greater sensitivity to the transmitter (postsynaptic) (Scott et al., 1976). Interestingly, anatomical studies demonstrated that motoneurons receive more synaptic contacts from homonymous than heteronymous Ia afferents (Burke et al., 1979; Burke et al., 1996);

which could be the underlying cause for the larger EPSP in the homonymous motoneurons.

Within the lumbar spinal cord there are rostro-caudal differences in EPSP strength for different motoneuron pools. For MG Ia afferents there are larger EPSPs in motoneuron pools relatively caudal within the lumbar spinal cord. For LG Ia afferents there are larger EPSPs rostral in the motoneuron pool within the lumbar spinal cord (Scott et al., 1976). This suggested that Ia afferent synaptic input varied as a function of position of the motoneuron. The larger EPSPs in specific regions of the spinal cord are thought to be due to a higher number of boutons per Ia afferent fiber on a given motoneuron (Scott et al., 1976). In summary, the number of synapses established by Ia afferents on a motoneuron is a major determinant of EPSP amplitude and therefore synaptic strength.

E1. VGLUT1 as a tool to recognize Ia afferent synapses: What is VGLUT1?

Ia afferents in the spinal cord form glutamatergic synapses with alpha motoneurons (Fyffe, 2001). Glutamate is synthesized from local precursors, such as glutamine released by glial cells, in the nerve terminals (Bear et al., 2006), and then is packaged inside synaptic vesicles. A brain-specific Na⁺-dependent inorganic phosphate transporter (BNPI) has been identified, using electron microscopy, in the synaptic vesicles of nerve terminals forming asymmetric excitatory synapses (Bellocchio et al., 1998). This protein was given the name vesicular glutamate transporter (VGLUT1) (Bellocchio et al., 2000). Vesicular glutamate transporter (VGLUT1) loads the glutamate

into small, clear vesicles that once packaged can be released at the synaptic cleft by exocytosis (Bear et al., 2006).

Differentiation-associated Na^+ -dependent inorganic phosphate dependent cotransporter (DPNI) is closely related to VGLUT1, localized to synaptic vesicles, and found to function as a glutamate transporter; this was the second isoform, VGLUT2 (Fremeau et al., 2001; Kaneko et al., 2002). Later a third isoform (VGLUT3) was cloned by screening cDNA libraries for homologous genes (Fremeau et al., 2002; Gras et al., 2002; Schafer et al., 2002).

Thus, three isoforms of the VGLUT transporter have been found, with VGLUT1 and VGLUT2 being most widely expressed in the spinal cord (Li et al., 2003; Oliveira et al., 2003; Todd et al., 2003; Alvarez et al., 2004; Landry et al., 2004). Different types of spinal cord glutamatergic synapses preferentially express one isoform over another (Li et al., 2003; Oliveira et al., 2003; Todd et al., 2003; Alvarez et al., 2004; Hughes et al., 2004; Landry et al., 2004). The functional differences between isoforms are not entirely clear; however, they have been used as markers to identify specific types of glutamatergic synaptic projections in specific brain areas. In this thesis VGLUT1 is used as a specific marker of Ia afferents in the ventral horn of the spinal cord.

E2. VGLUT1 as a tool to recognize Ia afferent synapses: VGLUT1 as a specific marker of proprioceptive synapses.

VGLUT1 synapses in the spinal cord are most frequently originated in sensory mechanoreceptors, including cutaneous and proprioceptors (Todd et al., 2003, Oliveira et al., 2003; Alvarez et al., 2004). In addition some descending inputs, like the corticospinal

tract, express VGLUT1 (Alvarez et al., 2004; Persson et al., 2006). VGLUT2 synapses originate mostly from spinal interneurons (Todd et al., 2003; Oliveira et al., 2003). VGLUT3 synapses occur at very low density and are considered to originate from some descending systems as no VGLUT3 expressing neurons are found in the spinal cord or the dorsal root ganglion (Oliveira et al., 2003). Here the evidence that VGLUT1 can be used in the ventral spinal cord as a marker of Ia afferents will be reviewed briefly.

An alternative marker to label proprioceptive Ia afferents during development is parvalbumin (PV). In mice, 95% of parvalbumin positive cells coexpressed the transcription factor Er81 specific of proprioceptors (Arber et al., 2000). Evidence derived from genetic experiments has shown that Er81 controls the projections of proprioceptors into the ventral horn (Arber et al., 2000). Parvalbumin positive synapses colocalize with the vesicular glutamate transporter 1 (VGLUT1) in the projection areas of proprioceptors in the rat spinal cord at age P5 (Alvarez et al., 2004). Mechanoreceptive afferents from the skin express high levels of VGLUT1 in lamina III-IV in the dorsal horn and are not parvalbumin positive (Alvarez et al., 2004). Parvalbumin is colocalized with VGLUT1 in the ventral horn and medial lamina V of the lumbar spinal cord in adult rats. Type Ib and type II afferents from muscle spindles project to medial lamina V and with Ia afferents are likely the origins of high levels of VGLUT1 in this region (Alvarez et al., 2004). Ia afferents additionally project to lamina VII and IX and are the likely origin of most VGLUT1 synapses in the ventral horn (Alvarez et al., 2004). Numerous approaches including: dorsal rhizotomies (Alvarez et al., 2004), anterograde tracing from dorsal roots (Mentis et al., 2006) and peripheral nerves (Todd et al., 2003), intracellular labeling of electrophysiologically identified Ia afferents (Alvarez, Bullinger, Cope,

unpublished), and depletion of VGLUT1 synapses from the ventral horn in Er81 knockout animals (Mentis et al., 2006) all strongly suggest that the large majority of VGLUT1 synapses found in lamina VII and lamina IX in rodents are originated in proprioceptors, mostly Ia afferents. Moreover, the peripheral sensory endings of Ia afferents around intrafusal muscle fibers also express VGLUT1 (Wu et al., 2004).

F1. Effects of peripheral nerve injuries: Synaptic stripping of motoneuron synaptic contacts

Removal of synaptic contacts in motoneurons axotomized due to peripheral nerve injuries was first observed in the rat facial nucleus (Blinzinger et al., 1968) and then confirmed in the rat hypoglossal nucleus (Sumner et al., 1973; Sumner, 1975), as well as in cat spinal motoneurons (Chen, 1978). An important observation in all of these studies is that axotomized motoneurons lose synaptic contacts around the cell soma and these changes are associated with an increase in microglial cells around the neuronal surface membranes. As soon as 2-4 days post-axotomy the microglia formed overlapping sheets of processes between neurons and synaptic terminals (Blinzinger et al., 1968; Kerns et al., 1973). Astrocytic processes increase, replacing the microglia at 2 weeks (Sumner et al., 1973; Chen, 1978) and peaking in number at 5 weeks (Sumner et al., 1973). At the same time the number and size of boutons decreases on the soma and dendrites (Sumner et al., 1973; Sumner, 1975; Chen et al., 1977; Chen, 1978).

There is significant depletion of total synaptic contacts on rat alpha motoneuron soma (75-88% depletion) and the proximal dendritic arbor (66-78% depletion) 3 weeks post-axotomy without regeneration (Linda et al., 2000). Different types of terminals had

varying levels of depletion; S-type (excitatory) terminals were depleted to a larger extent than F-type (inhibitory) terminals (Linda et al., 1992). The number of S-type excitatory synapses per 100 μm of soma membrane was also depleted in cat motoneurons by 70% 3 months after MG nerve axotomy without reinnervation (Brannstrom et al., 1998; Brannstrom et al., 1999). In these studies of cat motoneurons, F-type synapses were similarly depleted contrary to the work in rat motoneurons. The importance of differences in depletion between S and F-type boutons is the possibility of a shift in the ratio between the number of terminals that are excitatory as opposed to inhibitory (Linda et al., 1992).

Varying degrees of recovery were observed at 3 months post axotomy; from slightly to fully recovered depending on whether the synapse was inhibitory (F-synapses with flattened vesicles) or excitatory (S-synapses with spherical vesicles), (Sumner et al., 1973; Sumner, 1975; Chen et al., 1977; Chen, 1978). In the cat, S-type boutons recovered from 70% depletion of synaptic density on the cell soma (contacts per 100 μm of perimeter) to only 15% depletion after successful long term peripheral reinnervation following 3 months of axotomy without reinnervation. Surprisingly, F-terminal coverage did not recover in this study to the same extent and remained approximately 50% depleted 2 years after reinnervation (Brannstrom et al., 1998). None of these studies used specific markers for Ia afferent synapses; therefore, the fate of these synapses within the S-type group could not be directly analyzed.

To date, the synaptic contacts on the alpha motoneuron soma and proximal dendrites have been studied in great detail however the distal dendritic arbor has received less attention. Only the studies of Brannstrom and Kellerth (1998 and 1999) in the cat

analyzed synapses on dendritic arbors of axotomized motoneurons. The synaptic covering (area of postsynaptic membrane covered by synapses) and synaptic density of S-terminals (number of terminals per 100 μ m of membrane) targeting the proximal dendritic arbor (up to 100 μ m distance from the cell body) was depleted 24% and 28% respectively in 3 months post axotomy MG motoneurons that were prevented from reinnervating their peripheral targets. This reduction was small in comparison to the reductions in the cell body (70-78%) and reductions of F-terminals in proximal dendrites (72-78%). More distally, at 300 μ m and 700 μ m from the cell body, smaller depletions were observed in synaptic coverage (13 and 19%, respectively) or synaptic density (20 and 17%) of S-terminals. F-terminals showed no significant change at 300 μ m and were surprisingly increased at 700 μ m (27% in synaptic density and 36% in synaptic coverage). Two years after motoneuron reinnervation of the MG muscle, some recovery of synapses was observed. S-synapses showed a return to values similar to control in some compartments but not others; however, F-terminal coverage collapsed and remained decreased. Synaptic density of S-terminals was 5% increased up to 100 μ m from the cell soma but 20-25% decreased at 300 and 700 μ m from soma. F-terminal synaptic density was decreased compared to control by 35-40% at 100 μ m and 300 μ m from soma while only decreased 8% compared to control at 700 μ m from soma. Overall these complex patterns suggest that more work is necessary to clarify synaptic remodeling on motoneuron dendrites after axotomy. An important note on these studies (Brannstrom et al, 1998; Brannstrom et al, 1999) is that due to the time intensive nature of the electron microscopy methods used, the number of motoneurons analyzed for each time point and dendritic segment varied but was often very small (2-5 motoneurons) preventing statistical

comparisons. In the second study (Brannstrom et al, 1999), control data was not directly gathered but obtained from previous publications (Brannstrom et al, 1998). Thus, the data and conclusions from these papers must be confirmed in the future.

This thesis presents novel information on Ia afferent synapses on the motoneuron dendrites to the extent they could be labeled using a retrograde tracer, Cholera Toxin b subunit conjugated to Alexa 555 (CTb-555). Given the loss after peripheral nerve injury of excitatory synapses along with Ia-motoneuron EPSPs in motoneurons followed by partial recovery, a similar loss and recovery of Ia afferent synapses was expected. However, it is of note that Ia afferent synapses are injured; therefore, their behavior might be different when compared to other excitatory synapses originated in spinal interneurons or descending inputs which remain uninjured by peripheral nerve transections.

In addition, it is important to consider alterations of the dendritic arbor as a whole. Intracellular fills of motoneurons using HRP were initially used to study cell soma and dendritic changes in morphology after nerve injury. Cat alpha motoneuron soma size initially increased at 3 weeks post-axotomy before returning to normal size at 6-12 weeks post axotomy (Brannstrom et al., 1992). In hind limb motoneurons of the cat there is a decrease in dendritic diameter along with the membrane area and volume at all time points post-axotomy; amounting to a 30-50% decrease in total dendritic surface area of the alpha motoneuron at 3 months (Brannstrom et al., 1992; Linda et al., 1992). Therefore, changes in synaptic densities should be interpreted with an understanding of the morphological changes to the total dendritic arbor.

F2. Effects of peripheral nerve injuries: VGLUT1 contacts on alpha motoneurons in the spinal cord

One study analyzed changes in ventral horn VGLUT1 boutons after transection of the sciatic nerve (Hughes et al., 2004). Primary afferent terminals were anterogradely labeled in this study with CTb. VGLUT1 content of putative Ia afferent CTb labeled terminals that remain in lamina IX after sciatic nerve injury were progressively depleted 1, 2, 4 and 8 weeks post-injury to a maximum 65% decrease in luminance (Hughes et al., 2004). This study did not address synaptic stripping or whether these changes were reverted during reinnervation. In this thesis we directly investigated these important issues.

F3. Effects of peripheral nerve injuries: The monosynaptic reflex

Healthy cats were used to study the role of proprioceptive feedback in the regulation and adaptation of locomotor activity. Monosynaptic muscle afferent pathways in the spinal cord helped mediate the magnitude and duration of extensor/flexor activity along with disynaptic and polysynaptic muscle afferent pathways. This allowed for rapid adaptation in locomotion in response to unexpected loads and obstacles (Lam et al., 2002). Healthy adult male humans were used to study the independent control of joint stiffness; based on the changes in joint stiffness the monosynaptic stretch reflex was suggested to participate continuously during whole-limb equilibrium points (Latash, 1992).

Primates were used to study the inhibition of afferent sensory input to the spinal cord during voluntary movement. The Ia afferent input from the periphery onto the

spinal circuit varied; the input was either combined with descending motor input or suppressed to minimize interference. This study concluded that inhibition was presynaptic and therefore reduced the transmission at the initial synapse (Seki et al., 2003). Humans were used to observe change in the monosynaptic stretch reflex based on simple vs. difficult visuo-motor task. Similar to the previous study there was an increase in presynaptic inhibition of Ia afferents. Thus, presynaptic control of Ia afferents contributed to modulation of sensory inputs (Perez et al., 2005).

G1. Physiological recovery from peripheral nerve injury: Motor unit recruitment

Peripheral nerve injury results in dramatic alterations in motor performance that are recovered to different extents after reinnervation is complete in the periphery. Nerve sections in the human hand result in absence of orderly recruitment of muscle units (Thomas et al., 1987). Reinnervation re-established the size principle of motor unit recruitment as long as the motoneurons reinnervated the same muscle or a close synergist. Peripheral reinnervation restored voluntary control over muscle contraction; however, finely coordinated movement sequences remained impaired suggesting the importance of pattern recruitment for fine movement (Thomas et al., 1987). Similar studies in the cat on self-reinnervated MG nerves concluded that normal recruitment patterns recover when motoneurons successfully reinnervate the same muscles (Cope et al., 1993).

G2. Physiological recovery from peripheral nerve injury: Differences between self and cross reinnervation

Self-reinnervated hindlimb muscles in the cat, flexor digitorum longus (FDL) and soleus (SOL), exhibited normal locomotor activity patterns (O'Donovan et al., 1985). Interestingly, cross-reinnervated hindlimb muscles exhibited locomotor activity patterns associated with the innervating foreign motoneurons, suggesting that motoneuron activation and input patterns remain unaltered centrally (O'Donovan et al., 1985).

G3. Physiological recovery from peripheral nerve injury: Time course of reinnervation in the cat and rat

The time course for peripheral self-reinnervation in the cat had a rapid onset; however, motoneuron properties were altered and required more time to recover (Foehring et al., 1986b). After sectioning and self anastomosis of the MG nerve low reinnervation was observed from 5-6 weeks; at this time motoneuron properties were dramatically altered and there were no differences between motoneurons that elicited muscle contraction and those that did not. Medium reinnervation was from 9-10 weeks in which motor unit types recovered their normal electrical properties with a slight increase in firing rate (Foehring et al., 1986b). Following long term reinnervation, 10% of MG motoneurons elicited no contraction of the MG muscle, however the electrical properties in the remaining MG motoneurons as well as the proportion of each motor-unit type returned to control levels (Foehring et al., 1986a; Foehring et al., 1986b; Munson et al., 1986). In this thesis, the time-course for self-reinnervation after injuries to the tibial nerve in the rat was slightly accelerated with low reinnervation before 4 weeks (25%

reinnervation of neuromuscular junctions) and with high reinnervation at 8 weeks (>90% reinnervation of neuromuscular junctions) (Alvarez unpublished).

G4. Physiological recovery from peripheral nerve injury: Appropriate and inappropriate proprioceptive input in muscle after reinnervation

A self-reinnervated hindlimb muscle, medial gastrocnemius, in the cat was used to test the specificity of sensory reinnervation of cat skeletal muscle (Collins et al., 1986). The presence of field potentials in the homonymous motoneuron pool was used to determine afferent fiber type; Ia afferents were assumed to evoke field potentials in the motor group whereas Ib afferents were not (Collins et al., 1986). In a normal MG muscle 66% of the afferents innervated muscle spindles and 33% innervated golgi tendon organs (GTOs). In long term reinnervated MG muscles 50% of the afferents innervated muscle spindles, 33% were abnormal and did not innervate the muscle, and 10% innervated GTOs. This suggested that muscle spindles appeared to be reinnervated at random by former spindle and GTO afferents and that some of the connections were inappropriate. The inappropriate proprioceptive input could disrupt motor activity (i.e. locomotion). With time the improperly reinnervated receptors lost the ability to project to the homonymous motoneuron pool with a concurrent loss of field potentials (Collins et al., 1986).

G5. Physiological recovery from peripheral nerve injury: Loss of the stretch reflex

Despite regeneration of muscle afferents, self-reinnervated hindlimb triceps surae muscles in the cat show absent or significantly reduced stretch reflexes (Cope et al.,

1994). These results were then confirmed in the rat (Haftel et al., 2005). In self-reinnervated hindlimb muscles in the rat force production in the self-reinnervated muscles was restored; however, responses to the muscle stretch were not (Haftel et al., 2005). Surprisingly, the monosynaptic excitatory postsynaptic potentials (EPSPs) evoked by electrical stimulation of afferents on regenerated MG motoneurons were similar to normal (Haftel et al., 2005). Lack of proprioceptive feedback is reflected in the regulation of interjoint coordination during locomotion after peripheral nerve injury (Abelew et al., 2000; Maas et al., 2007). Small deficits were detected during level or up slope walking yet large deficits were detected during down slope walking. During down slope walking the coordination between the ankle and the knee was disrupted. This emphasized the importance of the stretch reflex for stiffness regulation during locomotion and implicated a possible loss of feedback from muscle spindle receptors as the cause of the deficit (Abelew et al., 2000). However, muscle spindle afferents were competent to encode muscle strength and transmit the monosynaptic excitation onto the motoneuron (Haftel et al., 2005). Despite the absence of length feedback, full recovery of kinematics in level and up slope walking suggested that proprioceptive loss was compensated by altered central drive or other sensory sources (Maas et al., 2007).

The behavioral consequence of areflexia could be due to multiple mechanisms. One of these is central suppression of sensory information from regenerated afferents, possibly by enhanced presynaptic inhibition of the Ia afferents sustained by segmental sources and/or enhanced by descending pathways. Alternatively, increase in postsynaptic inhibition could suppress the SSP of Ia afferent fibers without producing detectable

change in the motoneuron membrane potential in response to muscle stretch (Haftel et al., 2005).

In this thesis we investigate whether or not there are significant structural alterations in the Ia synapses themselves, such that the input to motoneurons is less effective. Previously it was reviewed that Ia synaptic strength of the Ia input is strongly dependent on the number of synapses and that these synapses can be labeled with VGLUT1. Therefore, we hypothesize that after peripheral nerve injuries regenerated motoneurons all show a significant change in the number or distribution of VGLUT1 contacts.

III. Specific Aims

Aim 1 analyzed VGLUT1 content in Lamina IX (LIX) of the spinal cord in rats with peripheral nerve injuries in which afferents and motor axons were allowed to reinnervate or were prevented from reinnervation. *The specific hypothesis is that after peripheral reinnervation VGLUT1 content in LIX recovers suggesting Ia afferent reconnection with axotomized motoneurons.* To test this hypothesis we estimated the density of VGLUT1 contacts on the cell soma of NeuN-immunolabeled motoneurons located in the LIX regions of the lumbar spinal cord containing motor pools with axons in transected and resutured tibial nerves (NeuN is a general neuronal marker). Changes in density were estimated at different post injury times from 3 days to 6 months. The results obtained falsified the hypothesis. Ia afferent somatic contacts were lost from the motoneuron cell soma and did not recover after peripheral regeneration.

Aim 2 analyzed changes in the density of VGLUT1 contacts on the cell bodies of MG motoneurons that specifically regenerated into the MG muscle. *The specific hypothesis is that recovery of VGLUT1 contacts might be improved in motoneurons that are reinnervating the appropriate muscles.* Tibial nerve injuries in aim 1 transected axons from multiple motoneuron pools targeting different muscle groups and it is possible that the motoneurons analyzed reinnervated inappropriate targets. To test whether motoneurons that reinnervate their original target show improved Ia afferent

connectivity we used a dual retrograde labeling approach to label MG motoneurons before injury (using Fast Blue retrograde tracer) and 1 week, 6 weeks, and 6 months after (using CTb 555). The results demonstrated that MG motoneurons reinnervating the MG showed a similar persistent loss of Ia synapses on their cell bodies.

Aim 3 analyzed changes in the density of VGLUT1 contacts on the dendritic arbor of MG motoneurons that regenerated into the MG muscle. According to existing literature, synaptic plasticity after peripheral nerve injuries might be different in the dendritic arbor than in the cell soma; the dendritic arbor receives over 90% of Ia afferent synaptic contacts. *The specific hypothesis is that VGLUT1 contacts in the dendritic arbor react differently from the cell soma after peripheral nerve injuries.* To test the hypothesis, the dendritic arbors of 8 FB and CTb-labeled MG motoneurons in each group analyzed in aim 2 (control, 1 week, 6 week, and 6 month post injury) were fully reconstructed using the NeuroLucida tracing system and VGLUT1 densities at different locations on the dendrite arbor analyzed. The results show that most of the VGLUT1 Ia afferents that are lost target the cell soma and proximal dendrites while little loss of synapses occurs in distal dendrites.

IV. Materials and Methods

A. Surgical Procedures

Animal procedures were carried out according to the NIH guidelines and were approved by the Laboratory Animal Use Committee of Wright State University.

Aim 1: Nerve Injuries.

The animal procedures in these experiments were performed before my arrival and therefore they are only explained briefly. Nerve injuries were similar to the procedures explained below. Fifteen adult Whistar rats had one survival surgery in which the tibial nerve was isolated, cut, and then either resutured as explained below in more detail, or ligated by placing a double tie in the proximal stump of the cut nerve. This tie prevented the injured axons from regenerating. The surgeries were performed by Dr. Timothy Cope and Paul Nardelli. The animals were euthanized with transcardial perfusions and prepared for histological analyses as explained below at 3 days, 1, 2, 4, 6, 12 weeks and 6 months post-injury. At each date only one animal was prepared except for 12 weeks nerve ligation in which two animals were prepared. Some animals were prepared for EMG recordings before sacrifice. All animals with resutured nerves and were older than 4 weeks post-injury showed EMG recovery. The materials were prepared by a previous graduate student Ms. Eileen Fitzsimons. I analyzed the materials with confocal microscopy as described more in depth below.

Aims 2 & 3: Retrograde labeling of control MG motoneurons.

Four control adult Whistar rats had one survival surgery for retrogradely labeling MG motoneurons with Cholera Toxin B (CTb) conjugated to the Alexa-555 fluorochrome. Each animal was anesthetized with Isoflurane; then the left leg was shaved and cleaned with 70% ethanol and betadine. A small incision was made with a scalpel on the midline of the left leg and skin separated from the muscle using the dissection scissors. The incision was extended rostrally to the division of the biceps femoris and caudally down to the ankle. The biceps femoris was reflected and the connective tissue around the lateral and medial gastrocnemius cleared. A microsurgery retractor was used to secure the biceps femoris. Several 2-5 μ L intramuscular injections of CTb 555 at 0.1% were distributed evenly throughout the medial gastrocnemius muscle totaling 6 μ L for animals 741-08-28 & 29 and 25 μ L for animals 741-09-61 & 62. Then the biceps femoris was closed using 4-O ethicon absorbable vicryl with a PS-5 needle in 3-4 sutures in an interrupted pattern. Then an interrupted subcutaneous closure of the skin was performed with surgical knots and irrigated with saline. All survival surgeries (these and those explained below) were performed by Lori Goss, RVT. An injection of .1 mL Buprenex was given intraperitoneal (IP) while the animal was anesthetized. This injection of .1mL Buprenex IP was the repeated every 12 hours for 48 hours. None of the animals showed signs of distress or pain.

The animals were transcardially perfused (procedure described below) with fixatives to collect the spinal cords 1 week after injecting the retrograde tracer.

Aim 2 & 3: Dual retrograde labelings and nerve injuries.

Animals were prepared and distributed into groups according to different post-injury survival time (1 week, 6 weeks and 6 months) and nerve injury (tibial or medial gastrocnemius nerve).

The first animal group (n=5 rats) had two survival surgeries and was used as the 1 week group. The first of the two survival surgeries was the same as the control survival surgery at a time point seven days before nerve injury (t= -7 days). In this case a total of 6 uL of CTb-555 at .1% were distributed evenly throughout the medial gastrocnemius muscle in 2-3 intramuscular injections. All other procedures were identical to those stated in the control group procedures. The second survival surgery implemented the nerve injury. Anesthesia and surgery proceeded as previously stated except that a Zeiss scope was now used to isolate the targeted nerve. For animal 741-08-30 the medial gastrocnemius nerve was isolated, cut, and resutured. For animals 741-08-42 through 45 the tibial nerve was isolated, cut, and resutured. Two sutures using 10-O ethicon were used to resuture the nerves through the epineurium. Then the wounds were closed and the animals postoperatively treated with Buprenex as before. The animals were transcardially perfused with fixative 1 week after the nerve injury.

The following animal groups had three survival surgeries and were the 6 weeks, 4 months, and 6 month groups. Six animals (2 MG injury, 4 Tibial injury) were prepared for the 6 week survival group. Two animals (only MG injury) were prepared for the 4 month survival groups (these data is not included). Eight animals (4 MG and 4 tibial injuries) were prepared for the 6 month survival group. The first of the three survival surgeries involved injecting Fast Blue to prelabel MG motoneurons 7 days before

peripheral nerve injuries ($t = -7$ days). The animals were anesthetized as before and the medial gastrocnemius muscle exposed as explained above. Several 5 μL intramuscular injections of Fast Blue 2.5% were distributed evenly throughout the medial gastrocnemius muscle totaling 25 μL . Then the wounds were closed and the animals treated post-operatively as previously stated. The second survival surgery was the nerve injury and was performed at a time considered $t = 0$ days. Animals were anesthetized and prepared as previously stated and the nerves cut and resutured using the same techniques. For animals 741-08-40 & 41, 741-08-56 & 57, and 741-09-70 through 73 the medial gastrocnemius nerve was isolated, cut, and resutured. For animals 741-09-64 through 67 and 741-09-81 through 84 the tibial nerve was isolated, cut, and resutured. The third survival surgery consisted in labeling regenerated MG motoneurons with CTb 555 and was performed at $t = 5.75$ weeks for 741-08-40 & 41 and 741-09-64 through 67; $t = 3.75$ months for 741-08-56 & 57; $t = 5.75$ months for 741-09-70 through 73 and 741-09-81 through 84. Intramuscular injections of .1% CTb 555 were evenly distributed throughout the medial gastrocnemius muscle totaling 6 μL for 741-08-40 & 41 and 25 μL for 741-08-57, 741-09-64 through 67, 741-09-70 through 73, and 741-09-81 through 84. Intramuscular injections of CTb 555 in animal 741-08-56 were at 5% and totaled 5 μL . The animals were transcardially perfused and fixed at 6 weeks, 4 months and 6 months after the nerve operations.

B. Tissue Preparation for analysis

Transcardial Perfusion with fixatives.

The animals were transcardially perfused and fixed with 4% Paraformaldehyde in 0.1 M phosphate buffer, pH 7.3 (PB). First, each animal was injected intraperitoneally (IP) with Euthasol at 2 μ L/g. Once deeply anesthetized, .05 mL of Heparin was injected through the retro orbital space into the bloodstream to prevent clotting during the perfusion. Then the thoracic cavity was opened and resected. A perfusion cannula was then inserted into the left ventricle and an incision made in the right atrium for drainage. The perfusates were pulsed using a peristaltic pump. First 50-100 ml of vascular rinse was used to clear the vascular system and push out all blood cellular elements. Then the aldehyde fixative (200-300 ml) was passed through the vascular system. The spinal cord (T1-S1) was then dissected out and placed in post fixation in the same fixative for 4 hours to overnight. The tissue was then cryoprotected by placing it into a solution of 15% sucrose in 0.1M PB at 4°C, overnight or until used.

Histological sectioning

The lumbar spinal cord was frozen in tissue freezing medium (OCT, Tissue Tek) and cut in a freezing sliding microtome. Transverse sections of the lower lumbar spinal cord (L4 to L6) were cut at 50 μ m thickness and collected free floating in .01 M PBS. All tissue sections were processed free-floating.

Immunolabeling

Aim 1. Spinal cord sections for all animals in Aim 1 (resutured and ligated) were immunostained for VGLUT1 using FITC-coupled secondary antibodies (green) and neuronal nuclear protein (NeuN) using Cy3-coupled secondary antibodies (red). The dual color immunolabelings were performed by Eileen Fitzsimons. The procedures are similar to those explained below. The NeuN antibody used was a commercially available (Chemicon) mouse monoclonal diluted 1:1,000 in .01M PBS. The VGLUT1 antibody was the same rabbit polyclonal antibody (Synaptic Systems) that was used in all other animals.

Aims 2 and 3. Spinal cord sections for control and 1 week survival animals in Aim 2 and 3 contained retrogradely CTb 555 (red) labeled motoneurons and were immunostained for VGLUT1 using FITC (green) as the label and counterstained with a Neurotrace blue Nissl (435 nm) to delineate laminar boundaries and motor pools. In all other animals, the sections contained Fast Blue MG motoneurons retrogradely labeled before the injury and CTb 555 labeled motoneurons that reinnervated the MG. These sections were immunolabeled for VGLUT1 using FITC (green) and counterstained with a deep red Neurotrace Nissl (640 nm).

After washing the sections in PBS to remove the excess of OCT freezing medium they were incubated in Neurotrace Nissl (Molecular Probes) for 30 minutes to 1 hour at a dilution of (1:100). Then the sections were blocked for 30 minutes to 1 hour with Normal Donkey Serum (NDS) diluted 1:10 in PBS with 0.1% Triton X-100 (PBS/TX). The sections were then placed in rabbit polyclonal antibodies against the Vesicular Glutamate Transporter 1 (VGLUT1, Synaptic Systems) diluted 1:1000 in PBS/TX and incubated

overnight at room temperature in continuous agitation on a rotatory orbital shaker. The next day the sections were thoroughly washed and the immunoreactive sites revealed with species specific secondary antibodies donkey anti-rabbit IgGs coupled to fluorescein isothiocyanate (FITC, Jackson labs) and diluted 1:50 in PBS/TX incubated for 2 hours at room temperature. All sections were then washed with 0.1M PBS, mounted on HistoBond slides (Fisher), cover slipped with Vectashield (Vector), and placed in a refrigerator at 6 degrees celsius until imaged.

C. Imaging and Analysis

Aim 1. Imaging was performed using confocal microscopy in an Olympus Fluoview (FV) 300 system and excited with line lasers of 488nm (VGLUT1-FITC) and 568nm (NeuN-Cy3). Low magnification images were obtained with the 10X objective and stacks of confocal optical sections separated by 2 μm z-steps collected throughout the thickness of the tissue section. High magnification confocal optical sections through individual NeuN-IR motoneuron somata were obtained using a 60X oil objective (N.A. 1.35) digitally zoomed X2. We obtained either a confocal stack through the whole cell body contained within the sections or sampled a few optical sections at mid-somatic levels that are well separated (at least 2-3 μm) so that the same VGLUT1-IR contacts did not appear in the different optical sections.

Aims 2 and 3. Imaging was performed using confocal microscopy in an Olympus FV1000 system and the sections excited with lasers lines of 405nm (Fast Blue and blue Nissl), 488nm (VGLUT1-FITC), 568nm (CTb 555), and 647nm (deep red Nissl). Low magnification images were imaged with a 10X objective and stacks of confocal optical

sections separated by 2 μm z-steps collected throughout the thickness of the tissue section. High magnification confocal stacks of individual CTb and/or Fast Blue motoneurons and their dendrites were obtained using a 60X oil objective (N.A. 1.35) digitally zoom X1 or X2 and a z-step of 0.5 μm .

Cell body analyses

Confocal optical sections were obtained throughout the cell body and analyzed with Fluoview software (Olympus). A mid-somatic optical section was identified as a region containing a well-developed nucleolus. In this section the number of VGLUT1 contacts was counted and the total cell body perimeter (excluding dendrites) was measured to obtain a linear density of VGLUT1 contacts per 100 μm . The same measurement was repeated in optical sections above and below the mid-plane cell body sections and separate by approximately 3-4 μm in the z-axis. Each animal average included data from 8-12 motoneurons in each defined motoneuron group. For animals that had retrograde tracers Fast Blue and CTb there were two groups of motoneurons analyzed. For the 6 week, 4 month, and 6 month groups of animals one group of motoneurons analyzed was Fast Blue only and the other had both Fast Blue and CTb. Cell body diameters (minimum, mean, and maximum) and surface areas of the 6 week and 6 month tibial nerve cut groups were obtained in Image Pro Plus 5.1 (Media Cybernetics). The images were exported from Fluoview and calibrated in Image Pro Plus 5.1. The average cell body somata of Fast Blue only motoneurons and dual labeled Fast Blue/CTb motoneurons were compared using a t-test.

Dendritic analyses

To obtain 3D reconstruction of VGLUT1 contacts on dendrites high magnification was necessary to discriminate the VGLUT1 contacts and at these magnifications the whole dendritic arbor could not fit within a single image. Therefore the full CTb-555 labeled dendritic arbors was imaged by obtaining four to six overlapping high magnification confocal stacks in the FV 1000 confocal microscope (magnification 60x1) that covered the full extent of the labeled dendrite. These images were then imported into the NeuroLucida confocal module and tiled in a single file to trace the cell soma and the full CTb-555 labeled dendrites. Neuron tracing was performed over several sessions in which cell bodies, dendrites, and VGLUT1 contacts were traced by moving up and down through a z-stack of confocal images. The perimeter of the cell soma was traced, with the reference point in the nucleolus of the cell, every 1 μm step in the z-stack and throughout the entire 50 μm thick cell section. From these reconstructions the NeuroLucida software calculated the somatic surface contained within the section. Not all motoneurons were fully contained within the section. In a majority of the motoneurons that were cut more than half of the cell body was contained within the section. To obtain a density of contacts the total number of VGLUT1-IR contacts was divided by the total amount of surface sampled.

Individual dendritic trees were manually traced from the proximal origin distally, varying in width of trace based upon CTb 555 labeling. Dendritic segments were traced by individual points that were more or less separated depending on the orientation of the dendrite or the tortuosity of its path. Section thickness was entered by adjusting the thickness of the cursor. From the length and thickness of the dendritic segments the

software calculated the dendritic surfaces and lengths. All branches of the dendritic arbor labeled with CTb 555 in the 50 μ m thick z-stack were traced. VGLUT1 contacts were then plotted on the soma and along the dendritic arbor in the correct z-section correlating to the contact surface. The number of VGLUT1 contacts was then normalized as per 10 μ m of linear dendrite or 100 μ m² of dendritic surface.

Sholl analysis was performed with NeuroLucida software through the formation of concentric rings centered around the soma and separated by 50 μ m of increasing distance. Total dendritic length and surface area within each ring was calculated. The number of VGLUT1 contacts was then normalized as per 10 μ m of linear dendrite or 100 μ m² of dendritic surface for all dendritic segments located within each 50 μ m concentric ring up to 250 μ m.

Statistics

Statistical analysis and graphing were performed with Excel (Microsoft), Sigma Stat 3.1 (Jandel), and Sigma Plot 9 (Jandel). One way ANOVA and t-test were respectively used for comparisons between groups and pairwise comparisons for synaptic density on the cell soma and dendritic arbor. Significance level was set at $p < 0.05$.

Figures

Plates were composed using Fluoview (FV) software, Image Pro Plus 5.1, and Corel Draw 11. Sharpening of some images was performed by applying a High Gauss filter in Image Pro Plus 5.1. Images were digitally retouched for brightness, contrast, and

gamma. None of the digital modifications altered the content of information within the images.

V. RESULTS

Aim 1:

Changes in VGLUT1 density around the cell soma of NeuN-labeled tibial pool motoneurons

VGLUT1 immunoreactivities (IRs) were compared in the spinal cords of rats with tibial nerve cuts that were followed by either a nerve resuture (to allow regeneration) or ligation (to prevent regeneration). A number of post-injury times were analyzed (3 days, 1, 2, 4, 6, 12 weeks and 6 months) to obtain the time course of depletion and possible recovery of VGLUT1 synapses. These animals were prepared and immunostained before my arrival and I completed their analysis (N=2 rats for 12 week ligated, N= 1 rat all other time points).

Analysis of Ia afferent synapses in tibial motoneuron pools of lamina IX (LIX) in low magnification (10X1) confocal images, using vesicular glutamate transporter 1 (VGLUT1) as a proprioceptive marker, revealed a decrease in overall VGLUT1-IR bouton density compared to the control side at all post-injury times from 1 week to 6 months, but not at 3 days after injury. Similar depletions were observed in the lumbar spinal cords of both resutured (reinnervated) and ligated (non-reinnervated) rats (Figure1). Additionally, the same sections were immunostained with NeuN and a large depletion of

Figure 1. Vesicular Glutamate Transporter (VGLUT1) Immunoreactivity (IR). VGLUT1-IR of the ventral horn in the lumbar spinal cord of rats with ligated and resutured tibial nerves at 3 days (A), 7 days (B), 12 weeks (C), and 6 months (D) post-injury. There is progressive depletion of VGLUT1-IR in lamina IX of the experimental side compared to control with time post-injury independent of whether there is reinnervation (resutured) or not (ligated). (LF) Lateral Funiculus, (VF) Ventral Funiculus, (LIX) Lamina IX.

Vesicular Glutamate Transporter 1-IR (VGLUT1-IR)

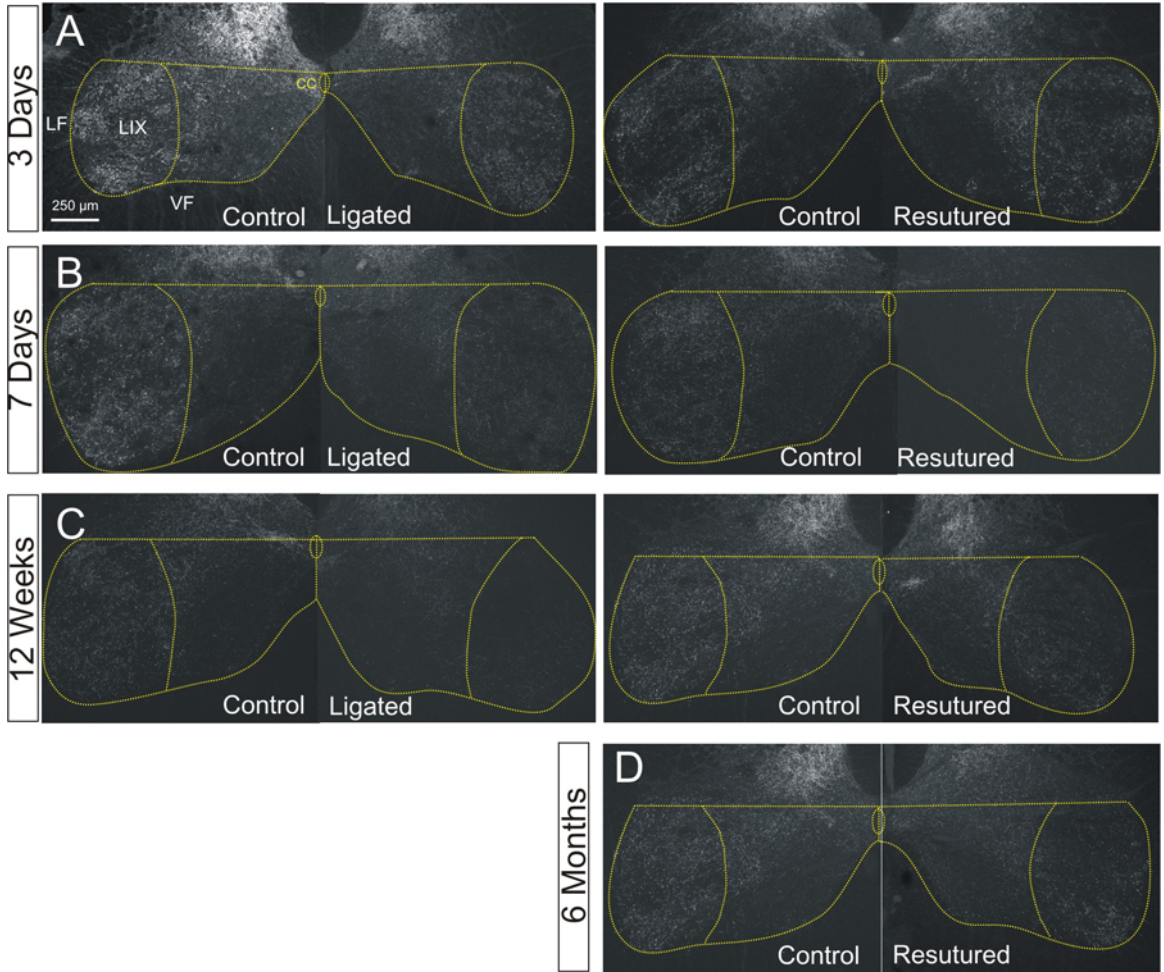
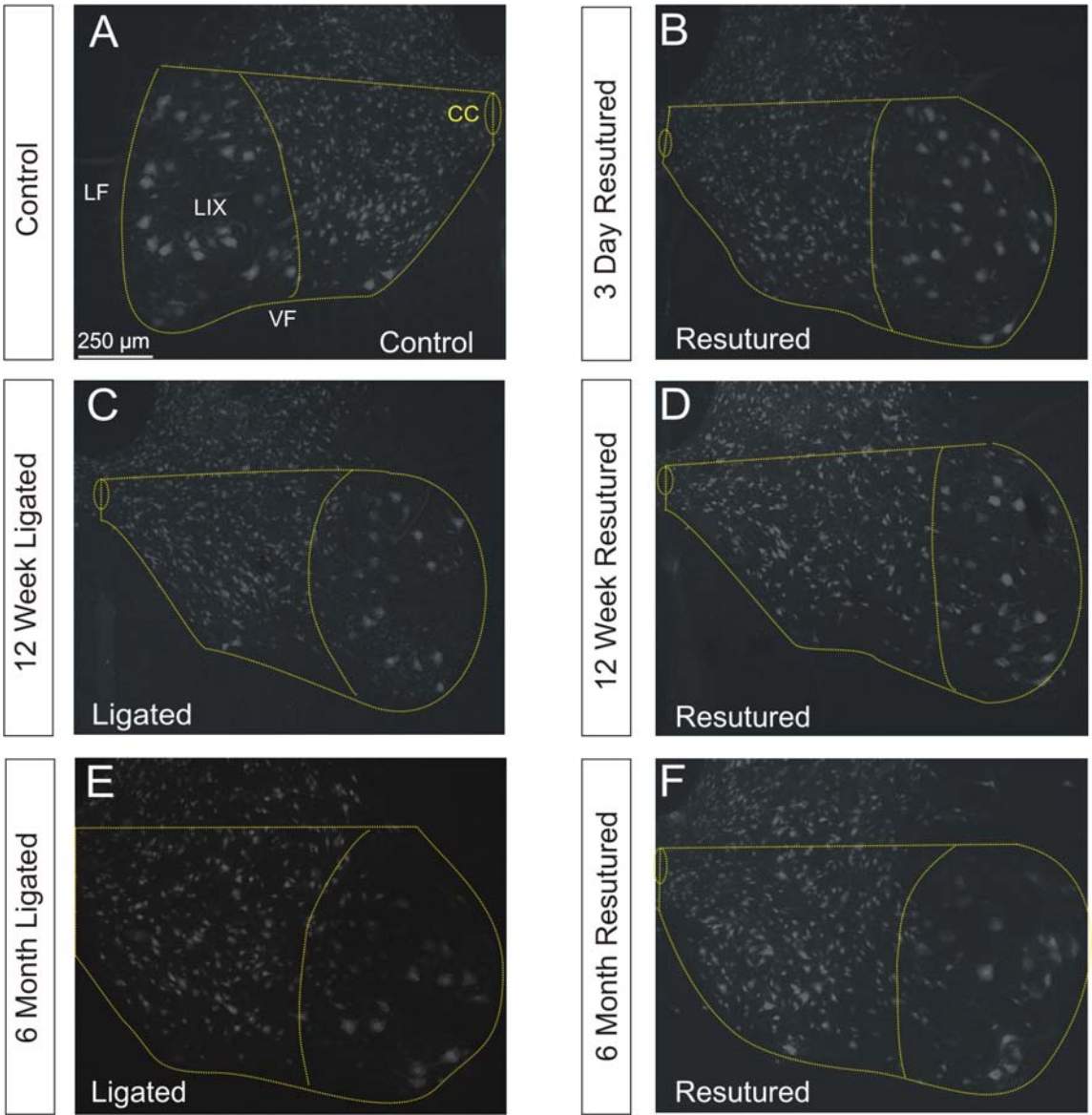


Figure 2. Neuronal Nuclear Protein-IR (NeuN-IR). NeuN-IR of motoneurons in lamina IX of the lumbar spinal cord of rats with ligated and resutured tibial nerves at 3 days (B), 12 weeks (C, D), and 6 months (E, F) post-injury. Decrease in intensity of NeuN-IR intensity was observed in all ligated and in early resutured rat motoneurons of the tibial pool in lamina IX of the experimental side (C-E) compared to control (A). In resutured rat motoneurons there was some recovery of NeuN-IR intensity of the tibial pool in lamina IX of the experimental side (F) compared to control (A) with long term reinnervation. (LF) Lateral Funiculus, (VF) Ventral Funiculus, (LIX) Lamina IX.

Neuronal Nuclear Protein-IR (NEUN-IR)



NeuN immunoreactivity in the cell somata of injured motor pools was observed (Figure 2). This was used to our advantage to identify the location of injured motoneurons for analyses.

NeuN-IR alpha motoneuron cell somata were imaged at high magnification (60X2) and through stacks of optical sections. The density of VGLUT1 contacts on NeuN-IR motoneuron cell somata within the tibial motoneuron pools of lamina IX (LIX) in the lumbar spinal cord was estimated by measuring 8-12 motoneuron cell bodies per animal. The density of VGLUT1 contacts on the cell soma was rather low; therefore, we imaged each motoneuron through at least three optical planes. This allowed us to sample on average 9.1 contacts per cell in control sides (range from 0 to 24). The results showed a decrease in the number of VGLUT1 contacts in the experimental (ipsilateral) side compared to the control (contralateral) side in spinal cords of rats that underwent a tibial nerve cut followed by resuture (reinnervation allowed) or a tibial nerve cut followed by ligation (reinnervation not allowed) (Figures 3 and 4).

No statistically significant differences in VGLUT1 density (contacts per 100 μm perimeter) on motoneuron cell somata were found between experimental (ipsilateral) compared to control (contralateral) side in the spinal cord of rats at 3 days post-injury for ligated (t-test $p=.99$) or resutured animals (t-test $p=.18$) (Figure 4A, 4B). At all later post-injury times there were statistically significant decreases in VGLUT1 density around alpha motoneuron cell somata in the experimental side compared to the control side of rats that were ligated and not allowed to regenerate; 7 days (t-test $p=.006$), 2 weeks (t-test $p<.001$), 4 weeks (t-test $p<.001$), 6 weeks (t-test $p<.001$), 12 weeks (t-test $p=.003$), and 6 Months (t-test $p=.002$) (see figure 4A) as well as in resutured rats; 7 days (t-test $p=.008$),

2 weeks (t-test $p=.013$), 4 weeks (t-test $p<.001$), 6 weeks (t-test $p<.001$), 12 weeks (t-test $p<.001$), and 6 months (t-test $p<.001$) (see figure 4B). Percent depletions in VGLUT1 density on experimental motoneurons compared to control slowly progressed from 34-40% 1 week post-injury to 80-90% at 4 weeks, independent of whether the animal was allowed to regenerate or not (Figure 4C, 4D). After 4 weeks and up to 6 months percent depletion remained stable and ranged from 75% to 96% in different animals. No statistically significant differences between resuture and ligated animals were apparent. In fact, the time-depletion curves were almost identical in both types of animals (Figure 4C).

Therefore, the results rejected the original specific hypothesis in that there was no recovery of VGLUT1-IR contacts lost around motoneurons cell bodies after peripheral nerve injuries and independent of regeneration and reinnervation of peripheral targets.

Figure 3. VGLUT1-IR and NeuN-IR for motoneurons within tibial motor pools.

VGLUT1-IR and NeuN-IR for motoneurons of rats with ligated and resutured tibial nerves at 3 days (A), 7 days (B), 12 weeks (C), and 6 months (D) post-injury. There is progressive depletion of VGLUT1-IR contacts on motoneuron cell somata within the tibial pools in lamina IX of the experimental side compared to control with time post-injury independent of whether there is reinnervation (resutured) or not (ligated). (N) Nucleus.

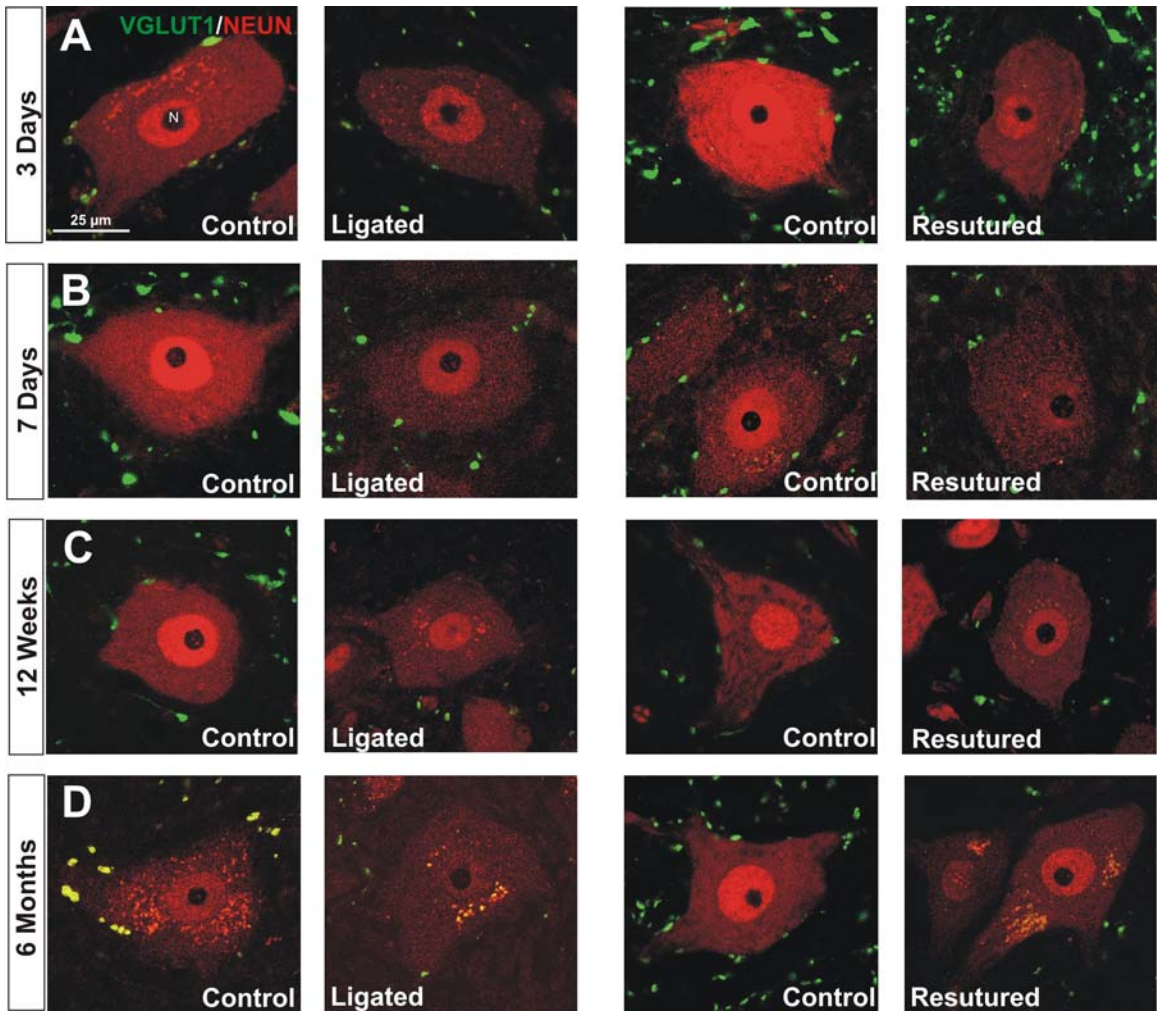
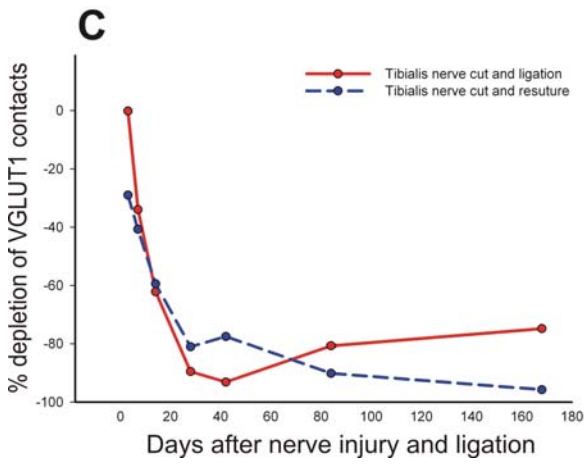
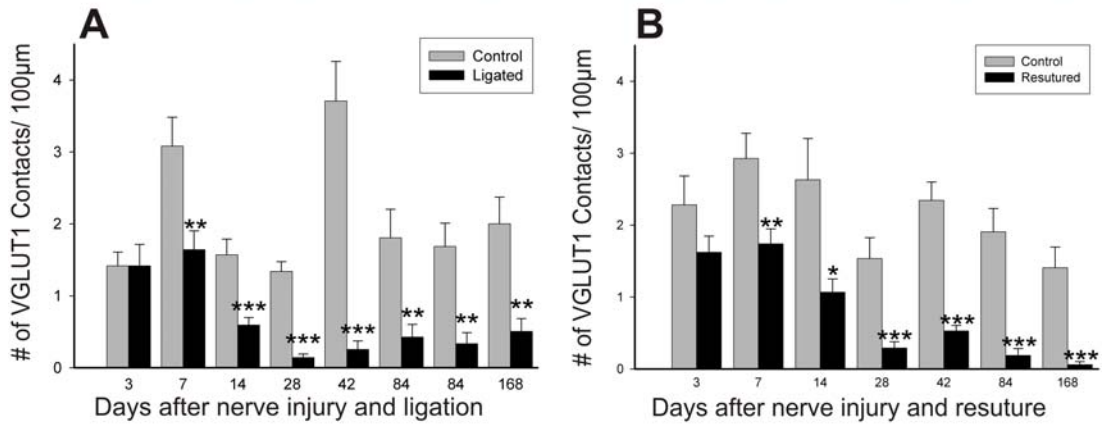


Figure 4. VGLUT1 contact densities on the cell soma of motoneurons in the Tibial motor pools. All motoneurons were immunolabeled with NeuN and Ia afferent synaptic contacts were immunolabeled with VGLUT1. Grey bars represent the average (+ SEM) VGLUT1 synaptic density in control motoneurons sampled from the contralateral side. Black bars indicate the VGLUT1 density on experimental motoneurons in the side ipsilateral to the nerve injury (A, B). (*) indicates significant change ($p < 0.05$, t-test). (A) Represents linear density of VGLUT1 contacts per 10 μm length of dendritic segment. (B) Represents surface density of VGLUT1 contacts per 100 μm^2 surface area of dendritic segment. (C) Time course of percent depletion of VGLUT1 synaptic density in experimental compared to the control. Percent depletions in VGLUT1 synaptic density were not significantly different between ligated (red line) and resutured (blue line) animals (D). There was never any recovery of VGLUT1 synaptic density.

VGLUT1 Contacts on the Soma of Motoneurons in the Tibial Pool



D

VGLUT1-IR Percent Depletion

	Ligated	N, rats	Resutured	N, rats
3 Days	-0.1	1	-29.0	1
7 Days	-34.0	1	-40.8	1
2 Weeks	-62.2	1	-59.4	1
4 Weeks	-89.5	1	-81.0	1
6 Weeks	-93.1	1	-77.5	1
12 Weeks	-80.7	2	-90.1	1
6 Months	-74.8	1	-95.7	1

Aim 2:

Changes in VGLUT1 density around the cell soma of retrogradely labeled MG

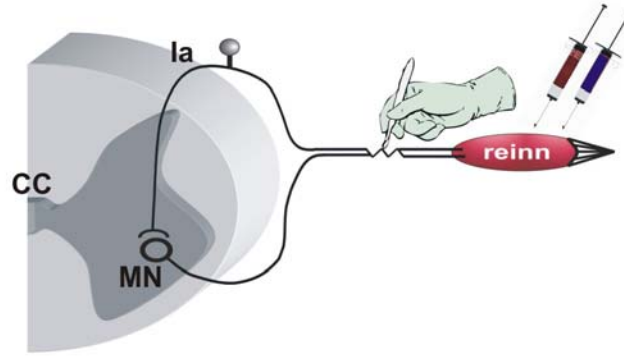
motoneurons

The tibial nerve injuries used in aim1 transected motor axons and primary afferents associated with several different motoneuron pools. No attempt was made to identify specific pools and it was possible that some of the motoneurons analyzed reinnervated inappropriate targets or did not innervate any targets at all. To test the specific hypothesis in aim 2 and specifically study motoneurons that reinnervated the appropriate target we utilized a dual retrograde labeling approach to label MG motoneurons before injury (using Fast Blue retrograde tracer) and 1 week (n=4 animals), 6 weeks (n=4), and 6 months (n=4) after injury (using CTb 555) using the same tibial nerve injury, cut and resuture model (Figure 5). In these animals dual Fast Blue and CTb 555 labeled motoneurons are MG motoneurons that properly reinnervated the MG. Fast Blue only motoneurons are more difficult to interpret; they could be MG motoneurons that failed to reinnervate the MG or neurons that failed to pick up the CTb tracer. Data was always compared to retrogradely labeled MG motoneurons from the control group (n=4). We analyzed on average 10.5 motoneurons (range 6-14) per animal in the four controls and all post-injury time groups.

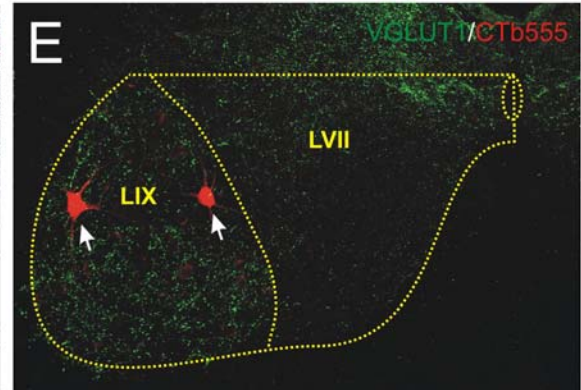
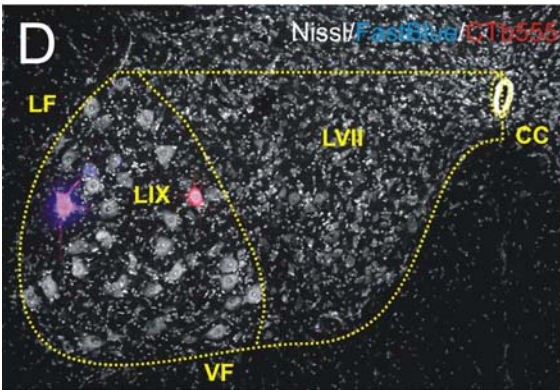
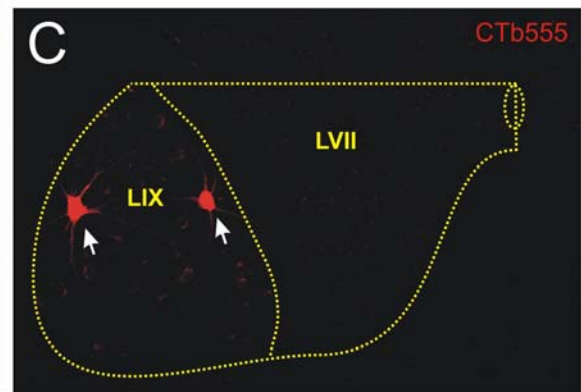
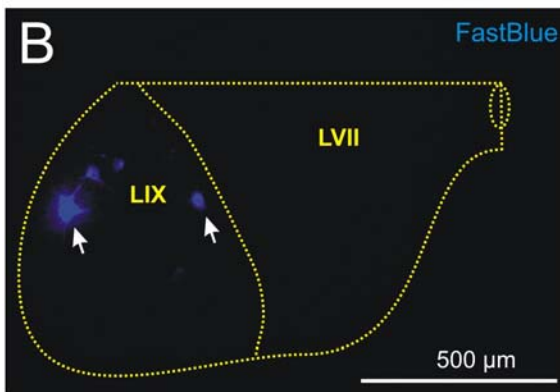
In a few animals we targeted the MG nerve for injury instead of the tibial nerve. The MG was resutured to allow for self-reinnervation. In these rats there was no possibility of inappropriate target reinnervation, however in these animals only homonymous Ia connections were injured while heteronymous connections were preserved. We studied 1 week (n=1) and 6 months (n=4) post-injury times. In these

Figure 5. Dual retrograde labeling for identification of appropriately reinnervated MG motoneurons. (A) Survival surgery timeline including injection of retrograde tracers and nerve injury time points. (B-E) Low magnification confocal images of retrogradely labeled motoneurons and VGLUT1 immunolabeled. Dotted lines indicate the ventral horn with a boundary around lamina IX. MG motoneurons retrogradely labeled with Fast Blue (FB) before the injury (B), retrogradely with Cholera Toxin B (CTb555) after the injury only (C), dual labeled with FB/CTb555 and counterstaining with Neurotrace Nissl (D), and the CTb 555 retrograde label with immunolabeled VGLUT1 contacts (E). Arrows indicate MG motoneurons that were labeled before injury (FB) and after injury (CTb555); indicating appropriate reinnervation in the MG muscle. (CC) Central Canal, (MN) Motoneuron, (Ia) Ia afferent fiber, (LF) Lateral Funiculus, (VF) Ventral Funiculus, (L) Lamina.

A



Group	T=-1	T= 0 (weeks)	T=+1	T= +5→+6	T=+25→+26
1 week	CTb 555	Cut & Resuture	analysis		
6 weeks	Fast blue	Cut & Resuture		CTb 555→analysis	
6 months	Fast blue	Cut & Resuture			CTb 555→analysis



groups we analyzed 10.6 motoneuron cell bodies per animal (range 6 to 18) and compared them to the uninjured control group (n=4) and to the 6 month tibial nerve injured group (n=4).

We confirmed the presence or absence of reinnervation in all animals with electromyography (EMG) (Figure 6). All 6 weeks and 6 month animals in the tibial or MG nerve injury groups showed successful reinnervation in the EMG records. In addition, in the 1 week post-injury tibial nerve cut animals one of the four displayed a small EMG. None of the 1 week post-injury MG nerve cut animals had an EMG present.

In agreement with the results in aim 1, the analyses in aim 2 revealed a significant decrease in the density of VGLUT1 contacts on MG motoneuron cell somata after tibial (Figure 7) and MG nerve injuries (Figure 8). Significant interanimal variability in VGLUT1 contacts density was detected within the 6 week and 6 month injury groups (Figure 7A; ANOVA, $p < 0.001$; significant differences indicated are after post-hoc Holm-Sidak pair-wise comparisons). In the control group one-way ANOVA comparison indicated the presence of significant differences among the groups ($p = 0.03$); however, post-hoc Holm-Sidak pairwise comparisons did not find any statistical differences between any two rats within the control group. Therefore, this difference might be due to a sampling problem between animals 1 and 3 (Figure 7A).

To investigate the cause of interanimal variability within the 6 week and 6 month group fast blue (FB) only motoneurons and FB/CTb dual labeled motoneurons were analyzed separately (Figure 7B and 7C). Fast Blue (FB) only labeled motoneurons showed no statistically significant differences 6 weeks post-injury (One-way ANOVA; $p = 0.12$); however, there was a significant difference in the 6 month post-injury group

Figure 6. Electromyography for reinnervated dual labeled MG motoneurons.

Electromyographs (EMGs) of the control group and experimental groups at 1 week, 6 weeks, and 6 months post-injury (cut and resuture). Only one rat of eight was slightly reinnervated at 1 week and belonged to the tibial nerve injury group. All 6 week and 6 month rats were reinnervated and had EMGs slightly smaller than the control. Group EMGs of experimental rats between MG and tibial nerve injuries were similar at all time points post-injury.

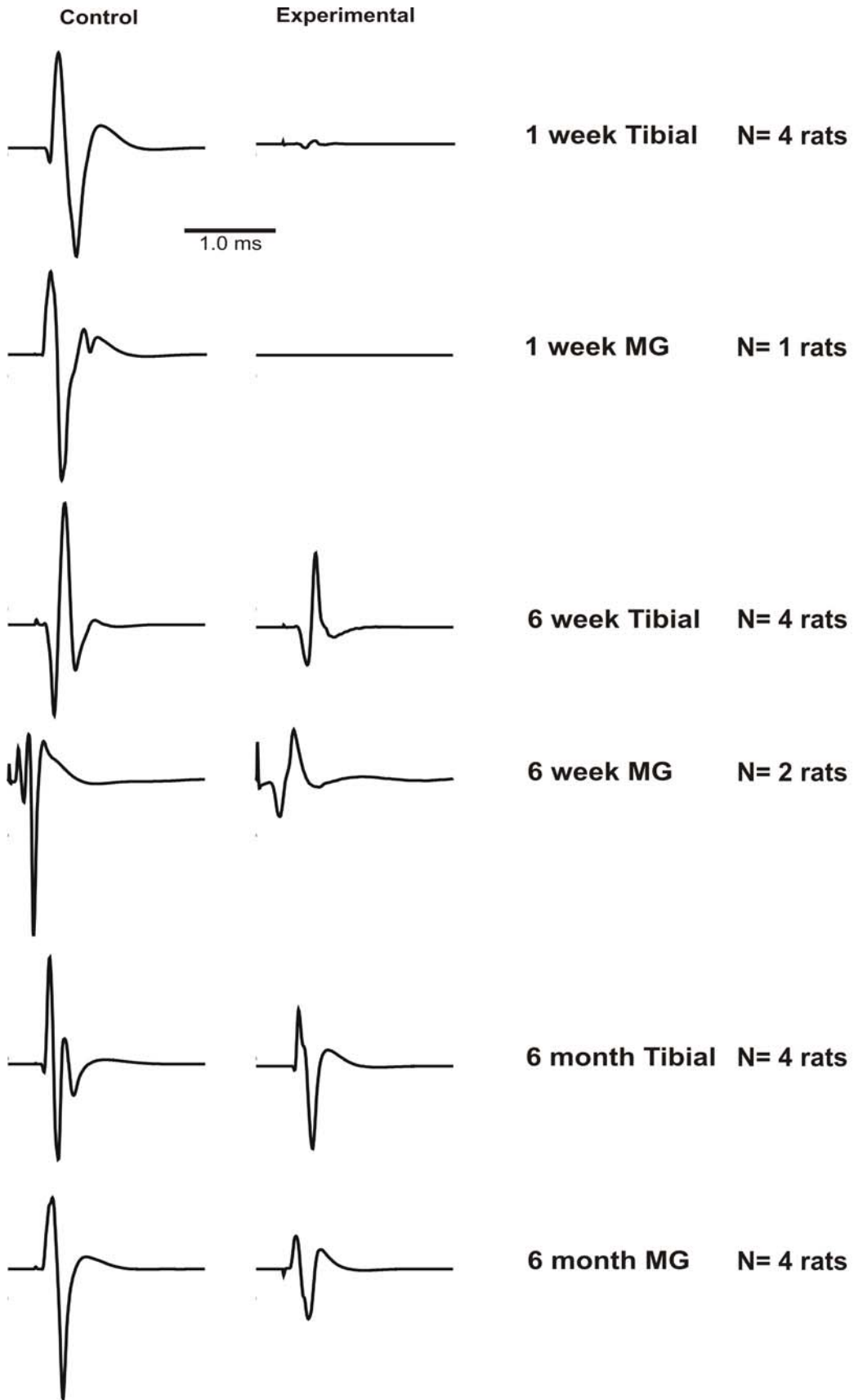


Figure 7. Density of VGLUT1 contacts on the soma of reinnervated MG motoneurons after tibial nerve cut and resuture. Bars represent the average (+ SEM) VGLUT1 synaptic density (A, B, C) for individual animals (N=8-12 motoneurons). There was interanimal variability between all motoneurons (A) and dual labeled motoneurons (C) in individual animals in the 6 week (3 of 4) and 6 month (4 of 4) groups. There was only interanimal variability between two animals for Fast Blue only labeled motoneurons (B) in the 6 month group. Bars represent the average (+ SEM) percent depletion VGLUT1 synaptic density compared to control group for groups of motoneurons within an animal (D). Most interanimal variability seems to arise from slightly better recovery of VGLUT1 density in MG motoneurons that successfully reinnervated the MG muscle in three of the eight animals. Bars represent the average (+ SEM) VGLUT1 synaptic density for a group of animals (N=4 rats) (E, F, G). There was extensive and permanent depletion of VGLUT1 contacts on the soma of motoneurons after peripheral nerve injury for motoneurons both appropriately reinnervated (F) and those that were not (E). There was not a significant difference at 6 weeks or 6 months between motoneurons that were appropriately reinnervated and those that were not (G). (*) indicates significant change ($p < 0.05$).

**Density of VGLUT1 contacts on the Soma of Reinnervated MG Motoneurons
After tibial nerve cut and resuture Individual Animal Analysis (N=8-12 Motoneurons)**

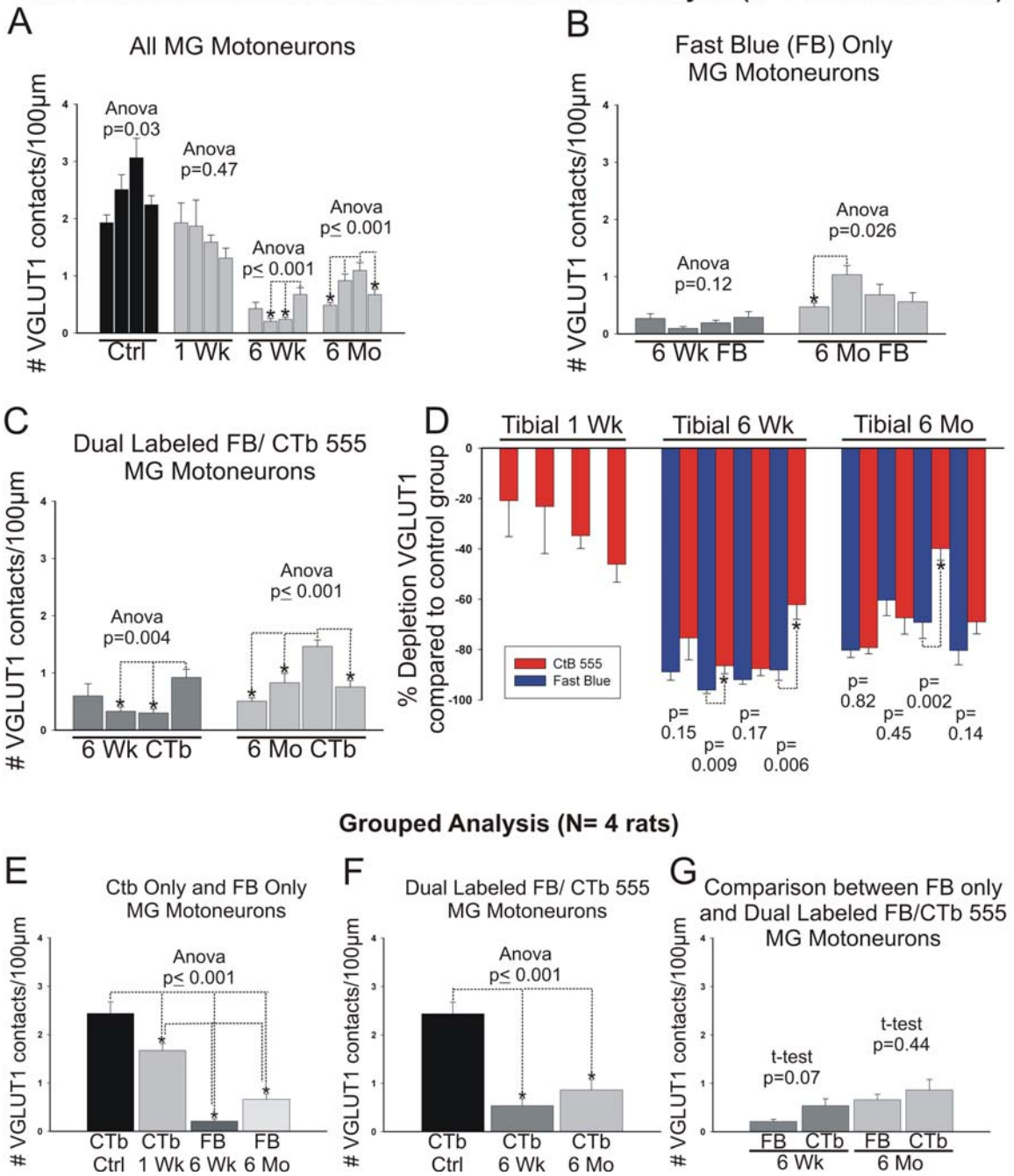
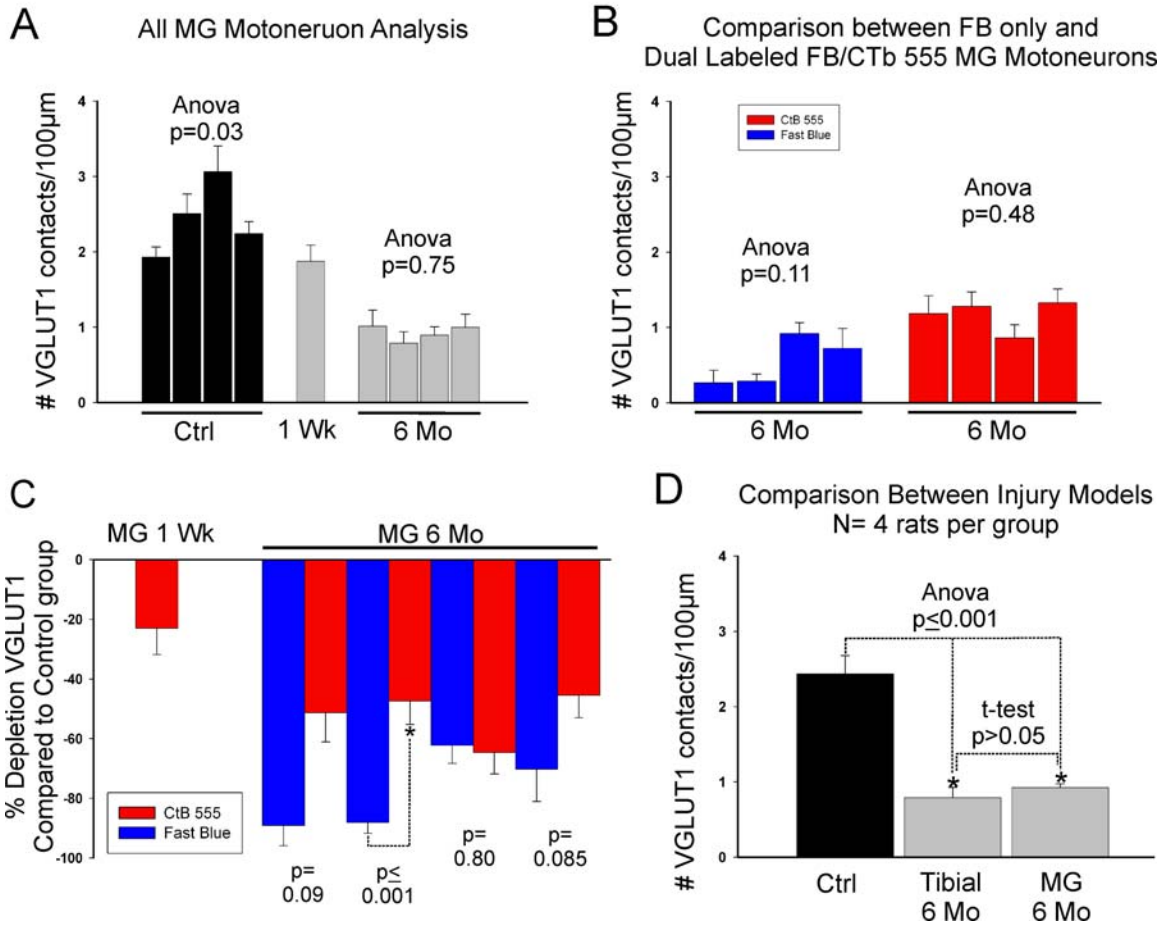


Figure 8. Density of VGLUT1 contacts on the soma of reinnervated MG motoneurons after MG nerve cut and resuture. Bars represent the average (+ SEM) VGLUT1 synaptic density (A, B) for individual animals (N=12 motoneurons). There was not interanimal variability between individual animals in the 6 month group. Bars represent the average (+ SEM) percent depletion VGLUT1 synaptic density compared to control group for groups of motoneurons within an animal (C). Interanimal variability seemed to arise from slightly better recovery of VGLUT1 density in MG motoneurons that successfully reinnervated the MG muscle in one of the four animals (C). Bars represent the average (+ SEM) VGLUT1 synaptic density for a group of animals (N=4 rats) (D). There was extensive and permanent depletion of VGLUT1 contacts on the soma of motoneurons after peripheral nerve injury after 6 months for both tibial and MG nerve cut (D). Comparing injury models, there was not a significant difference at 6 months between the tibial and MG nerve cut groups. (*) indicates significant change ($p < 0.05$).

**Density of VGLUT1 contacts on the Soma of Reinnervated MG Motoneurons
After MG nerve cut and resuture Individual Animal Analysis (N=12 Motoneurons)**



(One-way ANOVA; $p=0.026$). This was due to a significant difference between the animal with the largest average VGLUT1 density compared to the one with the lowest (post-hoc Holm-Sidak pairwise comparison, $p<0.05$). Interanimal variability was larger within FB/CTb dual labeled motoneurons in the tibial nerve injury group, finding statistically significant differences for both 6 week (One-way ANOVA; $p=0.004$) and 6 months rat (One-way ANOVA; $p\leq 0.001$) (Figure 7C). Holm-Sidak pairwise comparisons revealed statistically significant differences ($p<0.05$) in several animals within the 6 week and 6 month groups. However, interanimal variability was not observed after MG nerve injuries (Figure 8A).

When Fast Blue and dual labeled MG motoneurons were compared within single animals after tibial nerve injury and reinnervation, it was observed that in the 6 week and 6 month groups three out of the eight animals (two in the 6 week groups and one in the 6 month group) showed significantly less depletion of VGLUT1 density in dual labeled MG motoneurons compared to Fast Blue only labeled motoneurons (Figure 7D; t-tests $p<0.05$). When a similar comparison was made within single animals after MG nerve injury and it was observed that in the 6 month group 1 out of the 4 animals showed significantly less depletion of VGLUT1 density in dual labeled MG motoneurons compared to Fast Blue only labeled motoneurons (Figure 8C; t-tests $p<0.05$). In conclusion, most of the interanimal variability seems to arise from slightly better recovery of VGLUT1 density on the MG motoneurons that successfully reinnervated the MG muscle (Dual Fast Blue and CTb 555 labeled) in some animals compared to others.

Once interanimal variability within the sample was characterized an average was obtained for all four animals in each experimental group and comparisons were made for

changes at different post-injury times or in between Fast Blue only or dual labeled MG motoneurons. Significant decreases in VGLUT1 density were observed at all post-injury times compared to control (One-way ANOVA; $p < 0.001$) (Figure 7E). Moreover, post-hoc pairwise comparisons revealed further significant decreases from 1 week to 6 weeks and 6 months; however, no differences were detected between dual labeled MG motoneurons 6 weeks and 6 month post-injury (Figure 7F) suggesting lack of recovery even long-after peripheral reinnervation. No statistically significant differences within the 6 week (t-test; $p = 0.07$) and 6 month groups (t-test; $p = 0.44$) were found when comparing Fast Blue only and dual labeled motoneurons (Figure 7G) and similarly there were no statistical significant differences between Fast Blue labeled motoneuron at 6 weeks or 6 months post-injury.

A limited analysis of the MG nerve injury model was performed and included 1 week ($n = 1$ rat) and 6 month ($n = 4$ rats) time points (Figure 8). Statistical comparisons were only done with the 6 month MG nerve injury group. The results parallel those observed in the tibial nerve injury model (Figure 8A). Fast Blue labeled motoneurons frequently demonstrated lower density of VGLUT1 contacts for three animals. In this case, Fast Blue only MG motoneurons cannot be innervating inappropriate targets. Therefore, possible explanations can only be failure of retrograde transport of CTb 555 or lack of muscle reinnervation. Interestingly, no significant differences were found between tibial or MG injured motoneurons 6 months after injury (Figure 8D); perhaps suggesting that somatic VGLUT1 contacts are dominated by homonymous Ia inputs.

In conclusion, the cumulative analysis of the tibial and MG nerve injury models revealed a decrease in the density of VGLUT1 contacts on the cell somata of MG

motoneurons reinnervating the MG (dual labeled motoneurons) of 31.3% 1 week post-injury, 77.9% 6 weeks post-injury and 64.6% 6 months post-injury after tibial nerve cut and resuture and 55.2% 6 months after MG nerve injuries. These depletions are somewhat smaller than those estimated in aim 1 based on NeuN down regulation. One possibility is that each sampling strategy might have biased the results in a different direction; NeuN might be more down regulated in MG neurons with more limited recovery, while CTb labeling might favor neurons with more extensive recoveries. Nevertheless in both situations the depletions in VGLUT1 contacts on the cells somata were profound and did not significantly recover from 6 weeks to 6 months after peripheral reinnervation. Therefore we concluded that peripheral reinnervation does not lead to significant recovery of somatic VGLUT1 contacts.

Aim 3:

Changes in density of VGLUT1 contacts around the dendrites of retrogradely labeled

MG motoneurons

To analyze the changes in VGLUT1 contact density along the dendritic arbor we analyzed three-dimensional reconstructions, obtained with the NeuroLucida neuron tracing system (Figures 9 and 10), of the soma and dendritic arbors of 8 dual labeled (FB prior to injury and CTb 555 after regeneration) MG motoneurons in each experimental group (1 week, 6 week, and 6 month post-injury) in the tibial nerve cut model compared to control motoneurons that were labeled with CTb 555 only in uninjured animals (see Figure 10). We analyzed the linear and surface VGLUT1 densities in reconstructed neurons. Linear densities were calculated as total number of boutons per 10 μm of linear dendrite and surface densities were calculated as the number of boutons per 100 μm^2 of available surface. Surface density analyses take into account differences in dendritic diameter due to of distal tapering and the concurrent change in surface membrane available at more distant locations for dendritic segments of equal length. In each case we performed Sholl analyses in 50 μm bins of distance from the cell soma to analyze differences at different proximo-distal locations.

Proximal Sholl bin analysis revealed an average of 6 primary dendrites (range of 4-10) per motoneuron. This correlated with previous studies where an average of 8 primary dendrites (range of 6-12) per triceps surae motoneuron was observed (Chen et al., 1994). There was an average total dendritic length of 1,186 μm and an average total surface area of 14,105 μm^2 . In comparison to the fully labeled triceps surae motoneuron with a surface area of 147,000 μm^2 (Chen et al., 1994), only 10% of the total dendritic

Figure 9. 3D Analysis of Motoneuron VGLUT1 contacts. Retrogradely labeled control MG Motoneurons in the ventral horn visualized in stacked z-sections at low magnification (A) and at high magnification single z-section for the soma (B1, B2) as well as stacked z-sections for dendrites (C). The large arrow (A) points to a control MG motoneuron that is shown reconstructed below. Small arrows point to VGLUT1 contacts on the surface of the motoneuron (B1, B2, C). Analysis included overlapping high magnification panels in Neurolucida (D) with tracing up and down through the confocal stack along with plotting VGLUT1 contacts (E). The transverse image can be used for Sholl bin analysis (F). Filled circles represent VGLUT1 contacts on the surface of the motoneuron. (CC) Central Canal, (VF) Ventral Funiculus, (LF) Lateral Funiculus, and (L) Lamina.

3D Analysis of Motoneuron VGLUT1 contacts

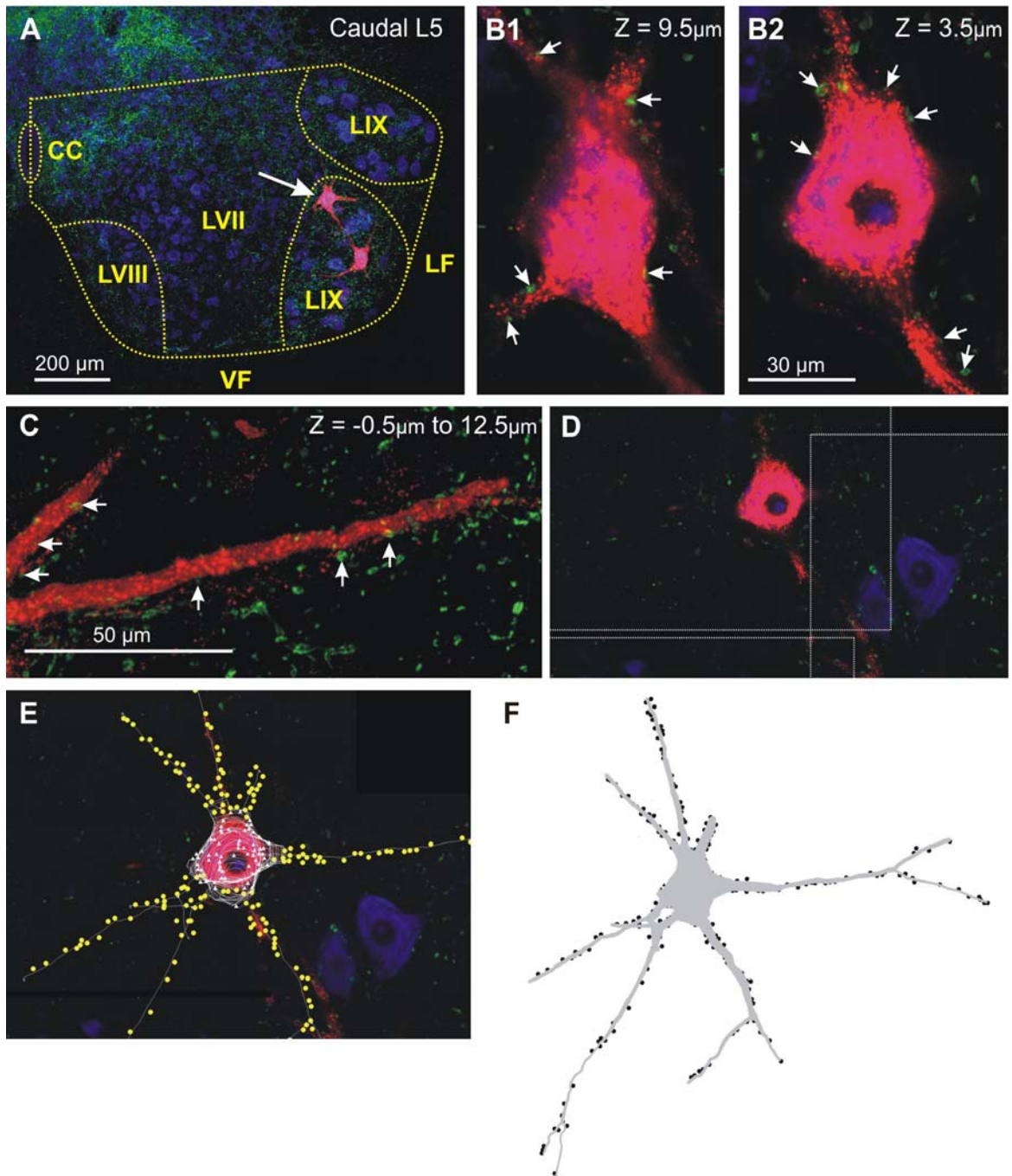
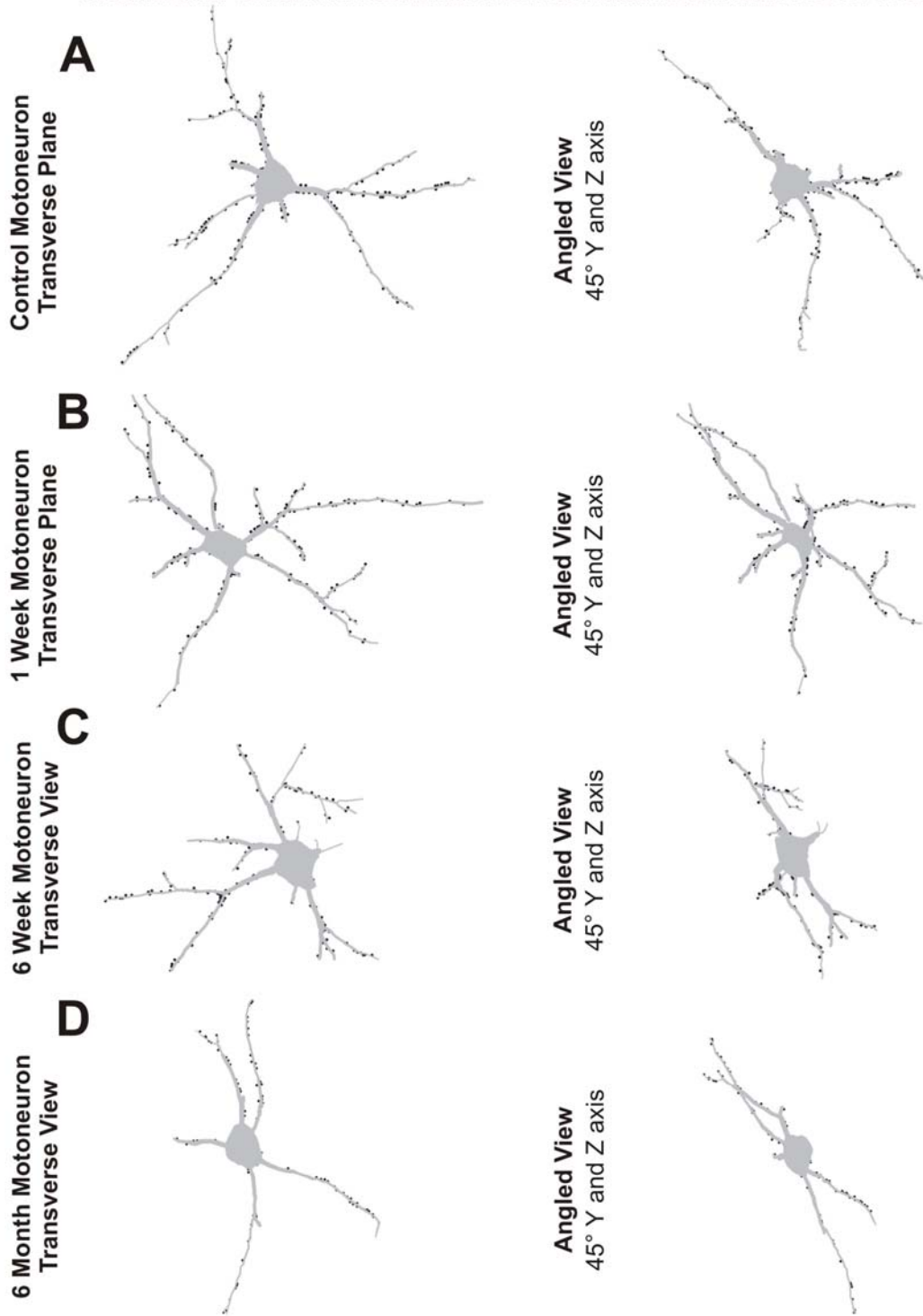


Figure 10. Motoneuron soma and dendritic arbor reconstructions showing VGLUT1 contacts. Reorganization of density of VGLUT1 contacts on the soma and dendritic arbor of appropriately reinnervated MG motoneurons. The control group (A) and 1 week (B) group of motoneurons were similar in linear and surface density throughout the dendritic arbor. However, proximal synaptic stripping was observed in the dendritic arbor in the 6 week (C) and 6 month (D) groups compared to the control.

Motoneuron Soma and Dendritic Arbor Reconstruction with VGLUT1 contacts



arbor was analyzed in this thesis. The average dendritic length sampled was 202.3 μm and the maximum dendritic length traced was 671.7 μm . In comparison to previous studies of fully labeled triceps surae motoneurons with an average dendritic length mediolaterally of 850 μm and dorsoventrally of 1350 μm (Chen et al., 1994), only 15-25% of the dendritic length was analyzed in this thesis. Existing studies in cat motoneurons have concluded that a majority of the dorsolateral and ventromedial Ia afferent contacts were within the first third (up to 500 μm) of the dendritic length (1600 μm) (Burke et al., 1996). Therefore, the 15-25% of dendritic length in the rat motoneuron analyzed in this thesis is well representative of the organization of the dendritic arbor for dendrites in these orientations. Limitations in analysis of the dendritic arbor were due to: orientation of the motoneurons within the transverse section, the thickness of the section (50 μm), and the incomplete fill of the distal dendritic arbor with CTb retrograde labeling.

The total CTb labeled dendritic arbor was used to calculate a total linear and surface dendritic densities of VGLUT1 contacts. However, due to the limited ability of the retrograde tracer to label distally located dendritic segments Sholl analysis in this thesis was only performed up to 250 μm from the soma to assure that all or the large majority of analyzed motoneurons and dendrites contained comparable number of dendritic segments at each distance.

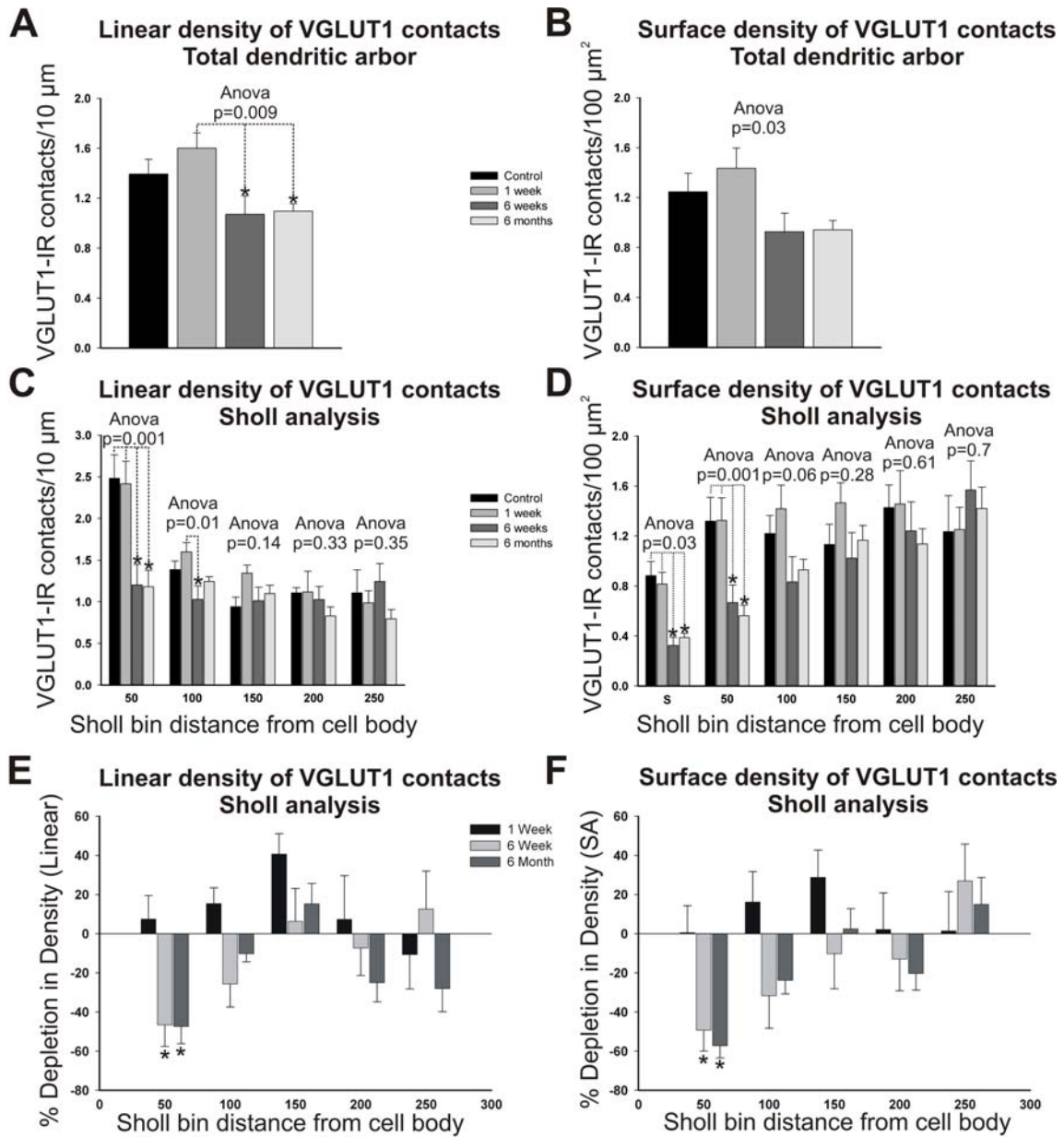
Overall there was a significant decrease in linear and surface VGLUT1 density in the whole dendritic arbor (One-way ANOVA; $p < 0.05$; Figure 11A and B). However, post-hoc analyses did not reveal statistical significant differences between injured

motoneurons and the control group. Therefore, if there are significant decreases in overall density they were too small to be evident within the present limited sample.

The absence of statistically significant change for the total dendritic arbor was mainly due to differences in distribution of VGLUT1 contacts located on proximal and distal dendrites. Sholl analyses revealed varying degrees of change in linear and surface density of VGLUT1 contacts in different dendritic compartments of MG motoneurons (Figure 11C and D). A significant decrease in linear VGLUT1 density compared to control (One-way ANOVA; $p < 0.001$) was detected in the first Sholl compartment 50 μm from soma of MG motoneurons 6 weeks and 6 months post-injury; yet not at more distal locations (Figure 11C). A similar result was obtained when considering surface densities (Figure 11D). In the second Sholl compartment, between 50 and 100 μm , a large depletion was consistently observed but compared to control the differences in VGLUT1 surface or linear density did not reach statistical significance. The percent decrease in VGLUT1 density was approximately 40 to 60% for surface and linear density in the first 50 μm from the soma in 6 weeks or 6 months animals and a 10 to 30% decrease at distances between 50 and 100 μm (Figure 11E and F). At more distal locations there were similar VGLUT1 densities between control and experimental animals. The one week group showed similar VGLUT1 density to controls in all dendritic compartments.

In conclusion, VGLUT1 losses were less marked on dendrites compared to cell bodies and the large majority of VGLUT1 contacts lost seemed to target the more proximal available surface on motoneurons in both soma and dendrites. As observed in the cell body, changes in density in proximal dendrites are permanent and do not recover even 6 months after reinnervation.

Figure 11. Density of VGLUT1 contacts on the soma of reinnervated MG motoneurons after tibial nerve cut and resuture. Bars represent the average (+ SEM) VGLUT1 linear (A) and surface (B) VGLUT1 synaptic density for groups of animals (N=8 motoneurons). Overall there was a significant decrease in linear and surface VGLUT1 density in the whole dendritic arbor; however, post-hoc analyses did not reveal statistical significant differences between injured motoneurons and the control group. Therefore, if there are significant decreases in overall density these were too small to be revealed within the present limited sample. A significant decrease in linear and surface VGLUT1 density compared to control was detected in the first Sholl compartment 50 μ m from soma of MG motoneurons 6 weeks and 6 months post-injury but not at more distal locations (11C, 11D). Bars represent the average (+ SEM) percent depletion VGLUT1 synaptic density compared to control group for groups of motoneurons within an animal (11E, 11F). The percent decreases in VGLUT1 density was between 40-60% for surface or linear density in 6 weeks or 6 months animals in the first 50 μ m from the soma and 10-30% decrease at distances between 50 and 100 μ m (11E, 11F). At more distal locations, there were similar VGLUT1 densities between control and experimental animals. The one week group showed similar VGLUT1 density to controls in all dendritic compartments. (*) indicates significant change ($p < 0.05$).



G

	Total	Sholl (50 μm)	Sholl (100 μm)	Sholl (150 μm)	Sholl (200 μm)	Sholl (250 μm)
	#/10 μm	#/10 μm	#/10 μm	#/10 μm	#/10 μm	#/10 μm
Control	1.3923	2.2482	1.3861	0.9542	1.1081	1.1051
1 Week	1.6009	2.4149	1.5987	1.3423	1.1885	0.9869
6 Week	1.0704	1.2014	1.0294	1.0139	1.0273	1.2442
6 Month	1.0967	1.1812	1.2439	1.0996	0.8302	0.7942

	#/100 μm^2	#/100 μm^2	#/100 μm^2	#/100 μm^2	#/100 μm^2	#/100 μm^2
Control	1.2469	1.3183	1.22	1.1392	1.4265	1.2355
1 Week	1.4354	1.3246	1.417	1.4665	1.4565	1.2526
6 Week	0.9168	0.668	0.8329	1.023	1.2413	1.5684
6 Month	0.9407	0.5634	0.9292	1.167	1.1367	1.4202

Conclusion

The analyses herein suggest reorganizations of VGLUT1 Ia afferent synapses on motoneuron somatodendritic surfaces after peripheral nerve injuries such that the input now targets more distal dendrites due to the loss and lack of recovery of the more proximal VGLUT1 synapses located in the cell somata and in the initial primary dendrite segments.

VI. DISCUSSION

The anatomical analyses revealed major reorganizations in the distribution and density of Ia synapses on motoneurons after peripheral nerve injuries. Synaptic stripping of Ia afferent synapses occurs mainly on the soma and proximal dendrites and appears to be permanent even after reinnervation. VGLUT1 synapses on more distal dendrites appear unchanged. These anatomical analyses compared to current physiological data can aid in understanding the absence of the stretch evoked synaptic potential (SSP) after peripheral nerve injury.

A1. Methodological Considerations: VGLUT1 as an effective marker of control and injured Ia afferent synapses

In this study, we used VGLUT1 to specifically label Ia afferent synaptic contacts in lamina VII and IX of the lumbar spinal cord. Numerous approaches including: dorsal rhizotomies (Alvarez et al., 2004), anterograde tracing from dorsal roots (Mentis et al., 2006) or peripheral nerves (Todd et al., 2003), intracellular labeling of electrophysiologically identified Ia afferents (Alvarez, Bullinger, Cope, unpublished) and depletion of VGLUT1 synapses from the ventral horn in Er81 knockout animals (Mentis et al., 2006) all strongly suggest that the large majority of VGLUT1 synapses found in the ventral horn in rodents originate in sensory afferents. We consider that the VGLUT1 synapses analyzed most likely originating from Ia afferents because no other sensory afferent projects that deep into the ventral horn. However, without more specific markers

we cannot exclude contributions from Ib and II afferents in the dendritic segments located in LVII. In previous studies, VGLUT1 immunoreactivity is dramatically reduced post-injury in anterogradely labeled proprioceptive afferents in lamina IX (Hughes et al., 2004). Therefore, one possible interpretation is that the reduced number of VGLUT1 contacts is due to loss of the marker, VGLUT1. However, anterogradely filled injured Ia afferents within the lumbar spinal cord contain the same level of VGLUT1-immunoreactivity as controls (Alvarez et al, 2008); therefore, the data presented is best interpreted as loss of the Ia afferent contact and not due to loss of the marker.

A2. Methodological Considerations: Large reductions in NeuN-labeled motoneuron versus MG retrogradely labeled motoneurons.

The depletions observed in NeuN-IR motoneurons were consistently larger than those observed in retrogradely labeled motoneurons. There is an early bias toward more depleted NeuN stained motoneurons because motoneurons were selected based on a decrease in intensity of staining. In the resutured animals, NeuN staining recovers. There is a bias towards less depleted dual retrogradely labeled motoneurons based on quality of staining which is activity dependent.

A3. Methodological Considerations: Extent of dendritic analysis

The dendritic analysis in this thesis was only for a portion of the total dendritic arbor of the MG motoneuron. There was an average total dendritic length of 1,186 μm and an average total surface area of 14,105 μm^2 . In comparison to the fully labeled triceps surae motoneuron with a surface area of 147,000 μm^2 (Chen et al., 1994), only

10% of the total dendritic arbor was analyzed in this thesis. The average dendritic length sampled was 202.3 μm and the maximum dendritic length traced was 671.7 μm . In comparison to the fully labeled triceps surae motoneuron with an average dendritic length mediolaterally of 850 μm and dorsoventrally of 1350 μm (Chen et al., 1994), only 15-25% of the dendritic length was analyzed in this thesis. Limitations in analysis of the dendritic arbor were due to: orientation of the motoneurons within the transverse section, the thickness of the section (50 μm), and the incomplete fill of the distal dendritic arbor with CTb retrograde labeling. Quantitative analysis could only be completed up to 250 μm from the soma for all of the motoneurons; therefore, we are only analyzing a quarter of the total dendrite. Previous studies in cat motoneurons revealed that a majority of the dorsolateral and ventromedial Ia afferent contacts were within the first third (up to 500 μm) of the dendritic length (1600 μm) (Burke et al., 1996). Hence, the 15-25% of the dendritic length of the rat motoneuron analyzed in this thesis is well representative of the organization of the dendritic arbor for dendrites at these orientations.

B. VGLUT1 contacts on the cell bodies of motoneurons are depleted after peripheral nerve injuries and do not recover.

The data presented estimated that 66-96% of VGLUT1 contacts on alpha motoneuron cell bodies are depleted (depending on time after injury and type of analysis) and there is no recovery even six months after injury, a time at which peripheral reinnervation has been completed according to EMGs. These data correlated with previous studies that suggest that 70% of S-type synapses are lost around the cell soma of motoneurons axotomized following peripheral nerve injuries (Brannstrom et al., 1998;

Linda et al., 2000; Hughes et al., 2004). In this sense, Ia afferent synapses and S-type synapses are similarly removed from the cell soma of motoneurons. However, in contrast to VGLUT1 synapses, S-type synapses are largely recovered after motoneurons reinnervate their peripheral targets (Brannstrom et al., 1999). We obtained similar results whether we analyzed linear densities on the perimeter of NeuN immunolabeled motoneurons or on the perimeter of MG motoneurons in which reinnervation of the MG muscle was confirmed by retrograde labeling. Moreover, a similar result was obtained when we analyzed VGLUT1 contacts as linear density on the perimeter of selected cell soma profile cross sections or when it was analyzed as surface density in a smaller sample of the whole reconstructed cell body. There were disparities in these estimates perhaps due to sampling differences (see above). Regardless, all confirmed a similar result: the somatic VGLUT1 contacts that are lost after peripheral nerve injuries do not recover or the recovery is very limited after peripheral reinnervation. Thus, differences in the behavior of the whole S-type population must have an alternative explanation. One important difference is that most S-type terminals are originated in interneurons and descending systems which are not damaged by the peripheral nerve injury, while VGLUT1-IR synapses from afferents were injured in the periphery.

Another important issue arises when comparisons are made between VGLUT1 contacts on the cell somata of MG motoneurons after tibial and MG nerve injuries. In the tibial nerve cut and resuture injury model, all Ia afferents that travel within the tibial nerve are affected; however, in the MG nerve cut and resuture injury model only MG Ia afferents are effected. Therefore, the MG alpha motoneurons in the MG nerve cut and resuture injury model have unaffected heteronymous afferents from the lateral

gastrocnemius and soleus muscles. It was surprising that there was not a statistically significant difference in the VGLUT1 density 6 months after injury between the tibial nerve and MG nerve injury models in the number of contacts around the cell somata. These data could suggest that homonymous contacts have a greater impact on central reorganization of the soma than heteronymous contacts. Further studies are needed on the origin of the contacts in order to corroborate this hypothesis.

Finally, significant interanimal variability of VGLUT1 density was detected in the tibial nerve groups, most frequently associated with appropriately reinnervated FB/CTb dual labeled alpha motoneurons, suggesting variability in strength of reinnervation of the MG afferents within the tibial nerve between animals. When Fast Blue and dual labeled MG motoneurons were compared within single animals, interanimal variability seemed to arise from slightly better recovery or smaller depletion of VGLUT1 density in MG motoneurons that successfully reinnervated the MG muscle in three of the eight animals for the tibial nerve cut animals and one of four MG nerve cut animals. Further analysis of electrophysiological data from these animals would be necessary to correlate strength of reinnervation with the extent of VGLUT1 depletion.

C. Reorganization of VGLUT1 contacts on the dendritic arbor.

In hindlimb alpha motoneurons, overall synaptic density decreases proximodistally along the dendritic arbor but the proportion of S-type (excitatory) synapses increase from soma to distal dendrites (Fyffe, 2001). In the rat, approximately 68% of VGLUT1 contacts on the traced dendritic arbor from 0-250 μm were proximal (0-100 μm from the soma) and 74.5% of total Ia contacts on the traced motoneuron were on the

soma and proximal dendrites (0-100 μ m from the soma). These data suggest that VGLUT1 contacts do not follow the same pattern as S-type contacts in rat MG motoneurons and Ia afferent synapses are more proximally concentrated than the overall S-type synapse population. A similar conclusion can be deduced from the data of Burke and Glenn (1996) in which most of the synapses in dorso-ventrally and ventro-medially oriented dendrites in the cat were found within the first third of the dendritic arbors (500-600 μ m distance from the cell body). In conclusion, it appears that a majority of VGLUT1 synapses are located in the dendritic regions most affected by stripping.

Interestingly, VGLUT1 contacts on dendritic segments located above 100 μ m from the cell soma seem to be relatively unaffected. Sholl analysis of linear VGLUT1 density (contacts per 10 μ m of dendrite) and surface VGLUT1 density (contacts per 100 μ m² of dendrite) revealed a central reorganization of VGLUT1 through proximal synaptic stripping of the dendritic arbor and preservation of contacts distally. Depletion in VGLUT1 surface synaptic density (57% from 0-50 μ m, 24% from 50-100 μ m) in the proximal dendritic arbor after 6 month appropriate reinnervation of MG motoneurons was similar to the trend of S-type linear synaptic density depletion (24 to 28% from 0-100 μ m) in the ligated nerve injury model in the cat (Brannstrom et al., 1998; Brannstrom et al., 1999); however, was dissimilar to the trend of S-type synaptic density recovery (a 5% increase from 0-100 μ m) in the long term reinnervated injury model in the cat (Brannstrom et al., 1998; Brannstrom et al., 1999). Therefore, these data suggest that recovery of proximal S-type synaptic contacts is not due to recovery of Ia afferent VGLUT1 contacts but from other S-type synaptic contacts.

In previous studies in the cat, S-type linear synaptic density remained 20% depleted at 300 μ m from the soma after peripheral nerve injury without reinnervation and remained 20-25% depleted at 300 μ m from the soma even with long term reinnervation (Brannstrom et al., 1998; Brannstrom et al., 1999). Notably, at more distal locations (100-250 μ m) there were similar VGLUT1 densities between control and experimental rats. Therefore, these data suggest sustained depletion of S-type synaptic contacts is not due to loss of VGLUT1 contacts but from other S-type contacts. In conclusion, VGLUT1 losses were less marked on dendrites compared to cells somata and the large majority of VGLUT1 contacts lost were proximally located in both soma and dendrites of motoneurons. Moreover, the behavior of VGLUT1-IR synapses on the dendritic trees of rat MG motoneurons does not correlate to that described for S-type synapses in cat MG motoneurons.

Thus, this thesis presents novel information on Ia afferent synapses on the dendritic trees of motoneurons to the extent that they could be labeled using retrograde labeling with Cholera Toxin b subunit conjugated to Alexa 555 (CTb-555). As observed in the cell body, changes in density in proximal dendrites are permanent and do not recover even 6 months after reinnervation.

D. Correlation of VGLUT1 contacts with the physiological changes observed in the Ia-motoneuron connection after peripheral nerve injury and regeneration.

Anatomical analysis after peripheral nerve injuries revealed major reorganizations in the distribution and density of Ia synapses over motoneuron; these changes appear to be relatively permanent. These anatomical analyses compared to current physiological

data can aid in understanding the absence of the stretch evoked synaptic potential (SSP) after peripheral nerve injury.

Despite regeneration of muscle afferents, self-reinnervated hindlimb triceps surae muscles in the cat and rat show absent or significantly reduced stretch reflexes (Cope et al., 1994; Haftel et al., 2005). Surprisingly, the monosynaptic excitatory postsynaptic potentials (EPSPs) evoked by electrical stimulation of afferents on regenerated MG motoneurons were similar to normal. The VGLUT1 contacts that appear to remain in distal dendrites are potentially responsible for these EPSPs; however, they appear to be unable to sustain the SSP.

Due to remote dendritic connections after peripheral nerve injury and reinnervation, dendritic filtering and electronic decay could have an effect on the ability to produce an effective synaptic current at the soma. This will be more significant for EPSPs arising at the soma asynchronously (as after an SSP) than synchronically fired by an electrical stimulus. Another possibility is central suppression of sensory information from regenerated afferents, possibly by enhanced presynaptic inhibition of the Ia afferents sustained by segmental sources and/or enhanced by descending pathways (Haftel et al., 2005). Alternatively, increase in postsynaptic inhibition could suppress the SSP of Ia afferent fibers without producing detectable change in the motoneuron membrane potential in response to muscle stretch (Haftel et al., 2005). Finally, there is the possibility that remaining VGLUT1-IR synapses arise from sensory synapses that are not connected to muscle spindles in the periphery. This possibility was highlighted recently by unpublished observations from Ms. Katie Bullinger and Dr. Timothy Cope in which the connection between single Ia afferents with a positive response to stretch in the

periphery and MG motoneurons was tested using the techniques of spike-trigger averaging after peripheral nerve injury followed by regeneration. It was found that in the large majority of pair recordings tested there was no EPSP found in between the Ia afferent and the motoneuron. Yet, in controls all pair Ia-motoneurons recordings displayed a connection. Whether the VGLUT1 contacts retained in distal dendrites are connected with a sensory afferent innervating a muscle spindle or not will need to be studied anatomically further in future studies.

Finally a critical note is that VGLUT1 contacts may be present anatomically yet not functional. Further analysis on the postsynaptic content of receptors will be required through electron microscopy to address this possibility.

In conclusion, the impact of the overall reorganization of synaptic contacts, resulting in a decrease in VGLUT1 on the soma and proximal dendritic arbor of the alpha motoneuron, is suggested to play a role in the strength of the central synaptic connection of the monosynaptic circuit. However, further anatomical and electrophysiological research is needed to understand the absence of the stretch reflex.

Bibliography

- Abelew, T. A., Miller, M. D., Cope, T. C., & Nichols, T. R. (2000). Local loss of proprioception results in disruption of interjoint coordination during locomotion in the cat. *Journal of Neurophysiology*, *84*(5), 2709-2714.
- Alvarez, F. J., Villalba, R. M., Zerda, R., & Schneider, S. P. (2004). Vesicular glutamate transporters in the spinal cord, with special reference to sensory primary afferent synapses. *The Journal of Comparative Neurology*, *472*(3), 257-280.
- Alvarez, F.J., Nardelli, P., Bullinger, K.L., Ukpabi, N., Crum, J.M., Zerda, R., Kraszpulski, M., & Cope, T.C. (2008) VGLUT1 content in central synapses of normal and regenerated Ia afferents. *Soc Neurosci Abstr* 74.1.
- Arber, S., Ladle, D. R., Lin, J. H., Frank, E., & Jessell, T. M. (2000). ETS gene Er81 controls the formation of functional connections between group Ia sensory afferents and motor neurons. *Cell*, *101*(5), 485-498.
- Bear, M. F., Connors, B. W., & Paradiso, M. A. (2006). *Neuroscience exploring the brain* (3rd ed.). Philadelphia, PA: Lippincott Williams & Wilkins.
- Bellocchio, E. E., Hu, H., Pohorille, A., Chan, J., Pickel, V. M., & Edwards, R. H. (1998). The localization of the brain-specific inorganic phosphate transporter suggests a

- specific presynaptic role in glutamatergic transmission. *The Journal of Neuroscience : The Official Journal of the Society for Neuroscience*, 18(21), 8648-8659.
- Bellocchio, E. E., Reimer, R. J., Fremeau, R. T., Jr, & Edwards, R. H. (2000). Uptake of glutamate into synaptic vesicles by an inorganic phosphate transporter. *Science (New York, N.Y.)*, 289(5481), 957-960.
- Blinzinger, K., & Kreutzberg, G. (1968). Displacement of synaptic terminals from regenerating motoneurons by microglial cells. *Zeitschrift Fur Zellforschung Und Mikroskopische Anatomie (Vienna, Austria : 1948)*, 85(2), 145-157.
- Brannstrom, T., Havton, L., & Kellerth, J. O. (1992). Changes in size and dendritic arborization patterns of adult cat spinal alpha-motoneurons following permanent axotomy. *The Journal of Comparative Neurology*, 318(4), 439-451.
- Brannstrom, T., & Kellerth, J. O. (1998). Changes in synaptology of adult cat spinal alpha-motoneurons after axotomy. *Experimental Brain Research. Experimentelle Hirnforschung. Experimentation Cerebrale*, 118(1), 1-13.
- Brannstrom, T., & Kellerth, J. O. (1999). Recovery of synapses in axotomized adult cat spinal motoneurons after reinnervation into muscle. *Experimental Brain Research. Experimentelle Hirnforschung. Experimentation Cerebrale*, 125(1), 19-27.
- Brown, A. G., & Fyffe, R. E. (1978). The morphology of group ia afferent fibre collaterals in the spinal cord of the cat. *The Journal of Physiology*, 274, 111-127.

- Brown, A. G., & Fyffe, R. E. (1981). Direct observations on the contacts made between ia afferent fibres and alpha-motoneurons in the cat's lumbosacral spinal cord. *The Journal of Physiology*, 313, 121-140.
- Burke, R. E., & Glenn, L. L. (1996). Horseradish peroxidase study of the spatial and electrotonic distribution of group ia synapses on type-identified ankle extensor motoneurons in the cat. *The Journal of Comparative Neurology*, 372(3), 465-485.
- Burke, R. E., Walmsley, B., & Hodgson, J. A. (1979). HRP anatomy of group ia afferent contacts on alpha motoneurons. *Brain Research*, 160(2), 347-352.
- Chen, D. H. (1978). Qualitative and quantitative study of synaptic displacement in chromatolyzed spinal motoneurons of the cat. *The Journal of Comparative Neurology*, 177(4), 635-664.
- Chen, D. H., Chambers, W. W., & Liu, C. N. (1977). Synaptic displacement in intracentral neurons of clarke's nucleus following axotomy in the cat. *Experimental Neurology*, 57(3), 1026-1041.
- Chen, X. Y., & Wolpaw, J. R. (1994). Triceps surae motoneuron morphology in the rat: A quantitative light microscopic study. *The Journal of Comparative Neurology*, 343(1), 143-157.
- Collins, W. F., 3rd, Mendell, L. M., & Munson, J. B. (1986). On the specificity of sensory reinnervation of cat skeletal muscle. *The Journal of Physiology*, 375, 587-609.

- Conradi, S. (1969). Ultrastructure of dorsal root boutons on lumbosacral motoneurons of the adult cat, as revealed by dorsal root section. *Acta Physiologica Scandinavica. Supplementum*, 332, 85-115.
- Conradi, S., Cullheim, S., Gollvik, L., & Kellerth, J. O. (1983). Electron microscopic observations on the synaptic contacts of group Ia muscle spindle afferents in the cat lumbosacral spinal cord. *Brain Research*, 265(1), 31-39.
- Cope, T. C., Bonasera, S. J., & Nichols, T. R. (1994). Reinnervated muscles fail to produce stretch reflexes. *Journal of Neurophysiology*, 71(2), 817-820.
- Cope, T. C., & Clark, B. D. (1993). Motor-unit recruitment in self-reinnervated muscle. *Journal of Neurophysiology*, 70(5), 1787-1796.
- Cope, T. C., Seburn, K., & Buck, C. R. (2001). How does nerve injury strengthen Ia-motoneuron synapses? In T. C. Cope (Ed.), *Motor neurobiology of the spinal cord* (pp. 271-304)
- Foehring, R. C., Sybert, G. W., & Munson, J. B. (1986a). Properties of self-reinnervated motor units of medial gastrocnemius of cat. I. long-term reinnervation. *Journal of Neurophysiology*, 55(5), 931-946.
- Foehring, R. C., Sybert, G. W., & Munson, J. B. (1986b). Properties of self-reinnervated motor units of medial gastrocnemius of cat. II. axotomized motoneurons and time course of recovery. *Journal of Neurophysiology*, 55(5), 947-965.

Freneau, R. T., Jr, Burman, J., Qureshi, T., Tran, C. H., Proctor, J., Johnson, J., et al.

(2002). The identification of vesicular glutamate transporter 3 suggests novel modes of signaling by glutamate. *Proceedings of the National Academy of Sciences of the United States of America*, 99(22), 14488-14493.

Freneau, R. T., Jr, Troyer, M. D., Pahner, I., Nygaard, G. O., Tran, C. H., Reimer, R. J., et

al. (2001). The expression of vesicular glutamate transporters defines two classes of excitatory synapse. *Neuron*, 31(2), 247-260.

Fyffe, R. E., & Light, A. R. (1984). The ultrastructure of group ia afferent fiber synapses

in the lumbosacral spinal cord of the cat. *Brain Research*, 300(2), 201-209.

Fyffe, R. E. (2001). Spinal motoneurons: Synaptic inputs and receptor organization. In T.

C. Cope (Ed.), *Motor neurobiology of the spinal cord* (pp. 21-46) CRC Press.

Gras, C., Herzog, E., Bellenchi, G. C., Bernard, V., Ravassard, P., Pohl, M., et al. (2002).

A third vesicular glutamate transporter expressed by cholinergic and serotonergic neurons. *The Journal of Neuroscience : The Official Journal of the Society for Neuroscience*, 22(13), 5442-5451.

Haftel, V. K., Bichler, E. K., Wang, Q. B., Prather, J. F., Pinter, M. J., & Cope, T. C.

(2005). Central suppression of regenerated proprioceptive afferents. *The Journal of Neuroscience : The Official Journal of the Society for Neuroscience*, 25(19), 4733-4742.

- Hughes, D. I., Polgar, E., Shehab, S. A., & Todd, A. J. (2004). Peripheral axotomy induces depletion of the vesicular glutamate transporter VGLUT1 in central terminals of myelinated afferent fibres in the rat spinal cord. *Brain Research*, *1017*(1-2), 69-76.
- Ishizuka, N., Mannen, H., Hongo, T., & Sasaki, S. (1979). Trajectory of group ia afferent fibers stained with horseradish peroxidase in the lumbosacral spinal cord of the cat: Three dimensional reconstructions from serial sections. *The Journal of Comparative Neurology*, *186*(2), 189-211.
- Kaneko, T., Fujiyama, F., & Hioki, H. (2002). Immunohistochemical localization of candidates for vesicular glutamate transporters in the rat brain. *The Journal of Comparative Neurology*, *444*(1), 39-62.
- Kerns, J. M., & Hinsman, E. J. (1973). Neuroglial response to sciatic neurectomy. I. light microscopy and autoradiography. *The Journal of Comparative Neurology*, *151*(3), 237-254.
- Lam, T., & Pearson, K. G. (2002). The role of proprioceptive feedback in the regulation and adaptation of locomotor activity. *Advances in Experimental Medicine and Biology*, *508*, 343-355.
- Landry, M., Bouali-Benazzouz, R., El Mestikawy, S., Ravassard, P., & Nagy, F. (2004). Expression of vesicular glutamate transporters in rat lumbar spinal cord, with a note on dorsal root ganglia. *The Journal of Comparative Neurology*, *468*(3), 380-394.

- Latash, M. L. (1992). Independent control of joint stiffness in the framework of the equilibrium-point hypothesis. *Biological Cybernetics*, 67(4), 377-384.
- Li, J. L., Fujiyama, F., Kaneko, T., & Mizuno, N. (2003). Expression of vesicular glutamate transporters, VGluT1 and VGluT2, in axon terminals of nociceptive primary afferent fibers in the superficial layers of the medullary and spinal dorsal horns of the rat. *The Journal of Comparative Neurology*, 457(3), 236-249.
- Linda, H., Cullheim, S., & Risling, M. (1992). A light and electron microscopic study of intracellularly HRP-labeled lumbar motoneurons after intramedullary axotomy in the adult cat. *The Journal of Comparative Neurology*, 318(2), 188-208.
- Linda, H., Shupliakov, O., Ornung, G., Ottersen, O. P., Storm-Mathisen, J., Risling, M., et al. (2000). Ultrastructural evidence for a preferential elimination of glutamate-immunoreactive synaptic terminals from spinal motoneurons after intramedullary axotomy. *The Journal of Comparative Neurology*, 425(1), 10-23.
- Luscher, H. R., & Clamann, H. P. (1992). Relation between structure and function in information transfer in spinal monosynaptic reflex. *Physiological Reviews*, 72(1), 71-99.
- Maas, H., Prilutsky, B. I., Nichols, T. R., & Gregor, R. J. (2007). The effects of self-reinnervation of cat medial and lateral gastrocnemius muscles on hindlimb kinematics in slope walking. *Experimental Brain Research. Experimentelle Hirnforschung. Experimentation Cerebrale*, 181(2), 377-393.

- Mentis, G. Z., Siembab, V. C., Zerda, R., O'Donovan, M. J., & Alvarez, F. J. (2006). Primary afferent synapses on developing and adult renshaw cells. *The Journal of Neuroscience : The Official Journal of the Society for Neuroscience*, 26(51), 13297-13310.
- Molander, C., Xu, Q., & Grant, G. (1984). The cytoarchitectonic organization of the spinal cord in the rat. I. the lower thoracic and lumbosacral cord. *The Journal of Comparative Neurology*, 230(1), 133-141.
- Moore, K. L., & Dalley, A. F. (Eds.). (2006). *Clinically oriented anatomy* (5th ed.). Baltimore, MD: Lippincott Williams & Wilkins.
- Munson, J. B., Foehring, R. C., Lofton, S. A., Zengel, J. E., & Sybert, G. W. (1986). Plasticity of medial gastrocnemius motor units following cordotomy in the cat. *Journal of Neurophysiology*, 55(4), 619-634.
- Nicolopoulos-Stournaras, S., & Iles, J. F. (1983). Motor neuron columns in the lumbar spinal cord of the rat. *The Journal of Comparative Neurology*, 217(1), 75-85.
- O'Donovan, M. J., Pinter, M. J., Dum, R. P., & Burke, R. E. (1985). Kinesiological studies of self- and cross-reinnervated FDL and soleus muscles in freely moving cats. *Journal of Neurophysiology*, 54(4), 852-866.
- Oliveira, A. L., Hydling, F., Olsson, E., Shi, T., Edwards, R. H., Fujiyama, F., et al. (2003). Cellular localization of three vesicular glutamate transporter mRNAs and proteins in rat spinal cord and dorsal root ganglia. *Synapse (New York, N.Y.)*, 50(2), 117-129.

- Perez, M. A., Lungholt, B. K., & Nielsen, J. B. (2005). Presynaptic control of group Ia afferents in relation to acquisition of a visuo-motor skill in healthy humans. *The Journal of Physiology*, 568(Pt 1), 343-354.
- Purves, D., Augustine, G. J., Fitzpatrick, D., Hall, W. C., Lamantia, A., McNamara, J. O., et al. (2008). *Neuroscience* (4th ed.). Sunderland, MA: Sinauer Associates, Inc.
- Purves, D. (1975). Functional and structural changes in mammalian sympathetic neurones following interruption of their axons. *The Journal of Physiology*, 252(2), 429-463.
- Schafer, M. K., Varoqui, H., Defamie, N., Weihe, E., & Erickson, J. D. (2002). Molecular cloning and functional identification of mouse vesicular glutamate transporter 3 and its expression in subsets of novel excitatory neurons. *The Journal of Biological Chemistry*, 277(52), 50734-50748.
- Scott, J. G., & Mendell, L. M. (1976). Individual EPSPs produced by single triceps surae Ia afferent fibers in homonymous and heteronymous motoneurons. *Journal of Neurophysiology*, 39(4), 679-692.
- Seki, K., Perlmutter, S. I., & Fetz, E. E. (2003). Sensory input to primate spinal cord is presynaptically inhibited during voluntary movement. *Nature Neuroscience*, 6(12), 1309-1316.
- Sumner, B. E. (1975). A quantitative analysis of boutons with different types of synapse in normal and injured hypoglossal nuclei. *Experimental Neurology*, 49(2), 406-417.

- Sumner, B. E., & Sutherland, F. I. (1973). Quantitative electron microscopy on the injured hypoglossal nucleus in the rat. *Journal of Neurocytology*, 2(3), 315-328.
- Swett, J. E., Wikholm, R. P., Blanks, R. H., Swett, A. L., & Conley, L. C. (1986). Motoneurons of the rat sciatic nerve. *Experimental Neurology*, 93(1), 227-252.
- Thomas, C. K., Stein, R. B., Gordon, T., Lee, R. G., & Elleker, M. G. (1987). Patterns of reinnervation and motor unit recruitment in human hand muscles after complete ulnar and median nerve section and resuture. *Journal of Neurology, Neurosurgery, and Psychiatry*, 50(3), 259-268.
- Todd, A. J., Hughes, D. I., Polgar, E., Nagy, G. G., Mackie, M., Ottersen, O. P., et al. (2003). The expression of vesicular glutamate transporters VGLUT1 and VGLUT2 in neurochemically defined axonal populations in the rat spinal cord with emphasis on the dorsal horn. *The European Journal of Neuroscience*, 17(1), 13-27.
- Wu, S. X., Koshimizu, Y., Feng, Y. P., Okamoto, K., Fujiyama, F., Hioki, H., et al. (2004). Vesicular glutamate transporter immunoreactivity in the central and peripheral endings of muscle-spindle afferents. *Brain Research*, 1011(2), 247-251.